### Title

Follicle-stimulating hormone-mediated decline in miR-92a-3p expression in pubertal mice Sertoli cells is crucial for germ cell differentiation and fertility




### Journal

Cellular and Molecular Life Sciences, 79(3)

### ISSN

1420-682X



### Authors

Gupta, Alka

Vats, Amandeep

Ghosal, Anindita

et al.



### Publication Date

2022-03-01

### DOI

10.1007/s00018-022-04174-9

Peer reviewed

Cellular and Molecular Life Sciences (2022) 79:136
https://doi.org/10.1007/s00018-022-04174-9

Cellular and Molecular Life Sciences

ORIGINAL ARTICLE

# Follicle-stimulating hormone-mediated decline in miR-92a-3p expression in pubertal mice Sertoli cells is crucial for germ cell differentiation and fertility

Alka Gupta[1,3] · Amandeep Vats[1] · Anindita Ghosal[1] · Kamal Mandal[1,4] · Rajesh Sarkar[1,5] · Indrashis Bhattacharya[1,6] · Sanjeev Das[1] · Rahul Pal[1] · Subeer S. Majumdar[1,2]

Received: 2 September 2021 / Revised: 25 January 2022 / Accepted: 27 January 2022 / Published online: 18 February 2022


## Abstract

Sertoli cells (Sc) are the sole target of follicle-stimulating hormone (FSH) in the testis and attain functional maturation post-birth to significantly augment germ cell (Gc) division and differentiation at puberty. Despite having an operational microRNA (miRNA) machinery, limited information is available on miRNA-mediated regulation of Sc maturation and male fertility. We have shown before that miR-92a-3p levels decline in pubertal rat Sc. In response to FSH treatment, the expressions of *FSH Receptor*, *Claudin11* and *Klf4* were found to be elevated in pubertal rat Sc coinciding with our finding of FSH-induced decline in miR-92a-3p levels. To investigate the association of miR-92a-3p and spermatogenesis, we generated transgenic mice where such pubertal decline of miR-92a-3p was prevented by its overexpression in pubertal Sc under proximal *Rhox5* promoter, which is known to be activated specifically at puberty, in Sc. Our in vivo observations provided substantial evidence that FSH-induced decline in miR-92a-3p expression during Sc maturation acts as an essential prerequisite for the pubertal onset of spermatogenesis. Elevated expression of miR-92a-3p in post-pubertal testes results into functionally compromised Sc, leading to impairment of the blood–testis barrier formation and apoptosis of pre-meiotic Gc, ultimately culminating into infertility. Collectively, our data suggest that regulation of miR-92a-3p expression is crucial for Sc-mediated induction of active spermatogenesis at puberty and regulation of male fertility.

✉ Subeer S. Majumdar
subeer@nii.ac.in; subeer@niab.org.in

1 Cellular Endocrinology Laboratory, National Institute of Immunology, Aruna Asaf Ali Marg, JNU Complex, New Delhi 110067, India

2 Present Address: Genes and Protein Engineering Laboratory, National Institute of Animal Biotechnology, Hyderabad, India

3 Present Address: Department of Molecular, Cell and Developmental Biology, University of California, Santa Cruz, USA

4 Present Address: Department of Laboratory Medicine, University of California, San Francisco, USA

5 Present Address: Department of Medicine, University of Chicago, Chicago, USA

6 Present Address: Dept. of Zoology, H. N. B. Garhwal University, Srinagar, Uttarakhand, India

**Graphical abstract**

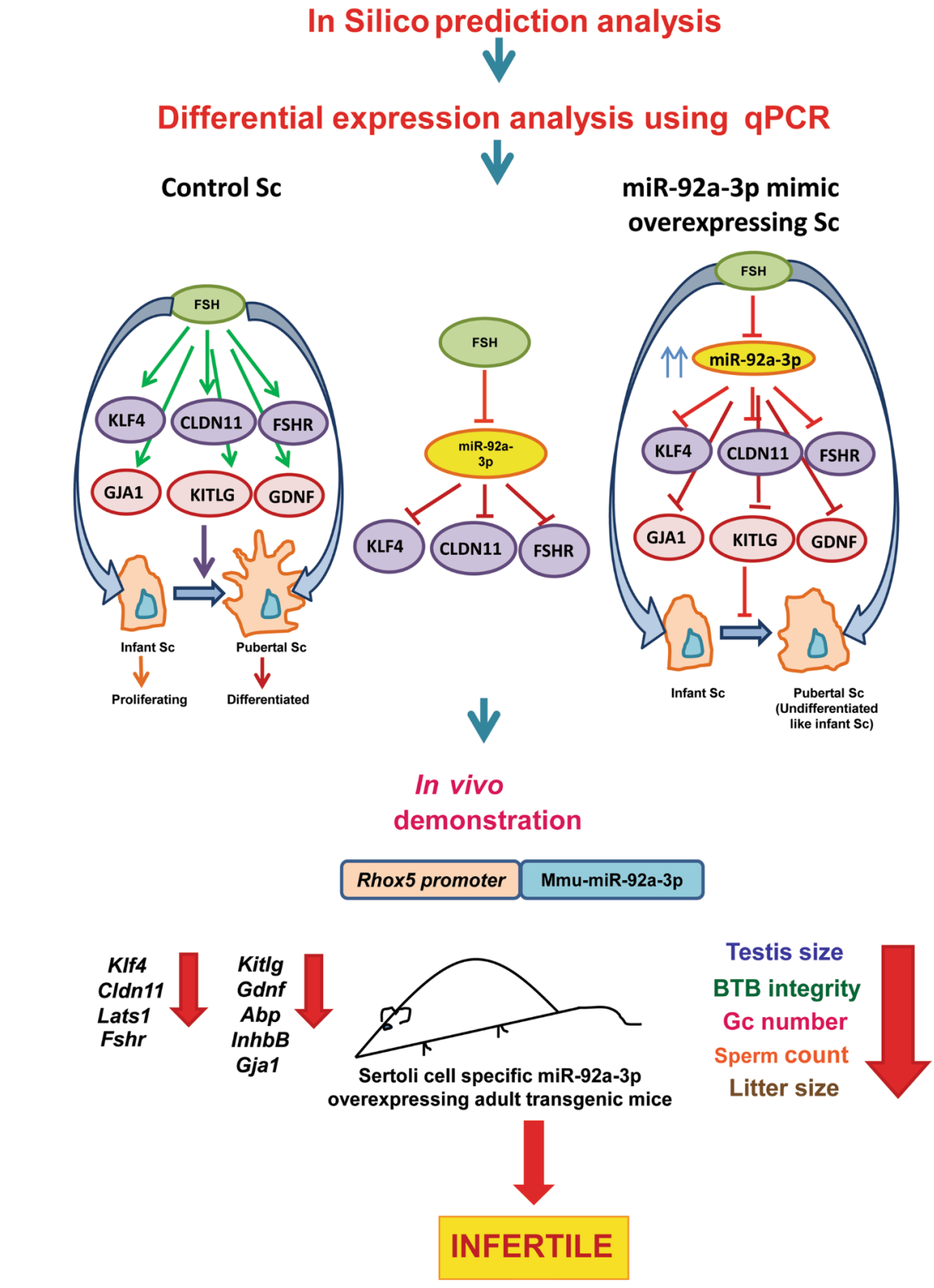

**Keywords** microRNAs · Sertoli cell · FSH · Spermatogenesis · Male infertility · Transgenic mice

## Introduction

During the past few decades, the semen quality has progressively deteriorated globally with an alarming decline in sperm counts [1–3]. Recent data indicate 1 in 20 men currently suffer from reduced fertility [4]. At least 30% of male infertility is idiopathic in nature with unknown aetiologies, thereby presently incurable by conventional hormonal supplementations [5]. Thus, there is an urgent need to understand the cellular and molecular events in the testes regulating sperm production [6–8]. The division and differentiation of male germ cells (Gc) to sperm occur inside the testicular seminiferous tubules under the tight control of gonadotropins—follicle-stimulating hormone (FSH) and luteinizing hormone (LH) [9, 10]. LH acts on the interstitial Leydig cells (Lc) to produce the testicular androgen—testosterone (T) [11]. Sertoli cells (Sc) are the major somatic cells of the seminiferous tubules that mature after birth and express the receptors for both FSH (FSH receptor, FSHR) as well as T (androgen receptor, AR), thus providing the micro-environment for Gc nourishment and differentiation [12, 13]. Sc offers structural support to all stages of the developing Gc and aids their movement from the basal compartment to the adluminal region of the seminiferous tubules [14]. This is achieved through the continuous remodelling of the tight junction proteins that form the immunological blood–testis barrier (BTB) [15]. Sc also provides the essential nutrients and nourishment necessary for Gc development [14]. Failure of Sc to perform any of the above functions negatively impacts male fertility.

FSH directs the expansion of Sc population during the neonatal/infantile period which determines the maximal spermatogenic capacity of the adult testes [16]. However during infancy, proliferative Sc remain incapable of responding adequately to the hormonal cues, which is necessary for the robust initiation of Gc differentiation [17–19]. Sc undergo functional maturation during pubertal testicular development with remarkable changes in hormonal signalling networks and transcriptome, leading to the establishment of BTB and robust initiation of Gc differentiation [20–22]. In pubertal Sc, FSH upregulates genes such as Kit ligand (*Kitlg)* or stem cell factor (*Scf*), glial cell-derived neurotropic factor (*Gdnf*), androgen-binding protein (*Abp),* Kruppel-like factor 4 (*Klf4*), etc., which are essential for spermatogenesis [20–25]. Mature Sc also produce inhibin B which inhibits FSH synthesis and secretion from the anterior pituitary [26]. Therefore, any defect in such hormonal cues during maturation of Sc adversely impacts the sperm production.

MicroRNAs (miRNA) are small non-coding RNAs (~ 22bps) that regulate the transcriptomic fate during cellular differentiation [27]. After being transcribed by RNA polymerase II, these small RNA fragments are processed by DICER and DROSHA to produce mature miRNA that binds to the 3' UTRs of the target transcripts, leading to their degradation or translational inhibition [28, 29]. Sc- or Gc-specific ablation of the DICER and/or DROSHA in mice has shown severe testicular defects leading to infertility [30–33]. Several studies have shown miRNAs such as miR-34/449, miR-10a, miR-100-3p, and miR-383 to be crucial for mammalian spermatogenesis [34–36]. Furthermore, patients with Sertoli cell only syndrome (SCOS) show an altered miRNA profile in the testis as compared to healthy fertile individuals [37]. The miRNA profiles differ substantially in immature and mature stages of testicular development in various mammalian species [38–40]. Since the causes of idiopathic male infertility, where hormones and signalling defects are ruled out in addition to obstructive causes, remain unknown, it is crucial to investigate this issue with new angles so that declining sperm count and male infertility both can be addressed appropriately.

In this present study, we intended to identify a microRNA which regulates the expression of various genes known to be essential for the functional maturation of Sc. In the semi-high-throughput screening of miRNAs in Sc reported previously by us, miR-92a-3p showed up as a promising candidate that is abundantly expressed in infant (5 days old) rat Sc, but declined naturally in pubertal (19 days old) rat Sc [41]. MiR-92a-3p belongs to the miR-17/92 cluster, which is one of the most studied miRNA clusters. Comprising a total of 15 miRNAs and four 'seed' families, these miRNAs have been studied for their role in cell proliferation, tumorigenesis, immunology, ageing, cardiovascular disease and neurodegenerative diseases [42, 43]. MiR-92a-3p targets genes such as *Klf4, Pten, Sirt1,* and *Rora* that play an important role in Sc maturation. However, there are no reports yet on miR-92a-3p-mediated regulation of Sc maturation or male fertility. Here, we have reported that miR-92a-3p directly targets genes such as *Cldn11* and *Fshr* that are crucial for Sc functioning. To evaluate the association between the developmentally altered expression pattern of miR-92a-3p in Sc and spermatogenesis, we generated a novel transgenic mouse model with persistent expression of miR-92a-3p in adult Sc without any decline. These results demonstrate the

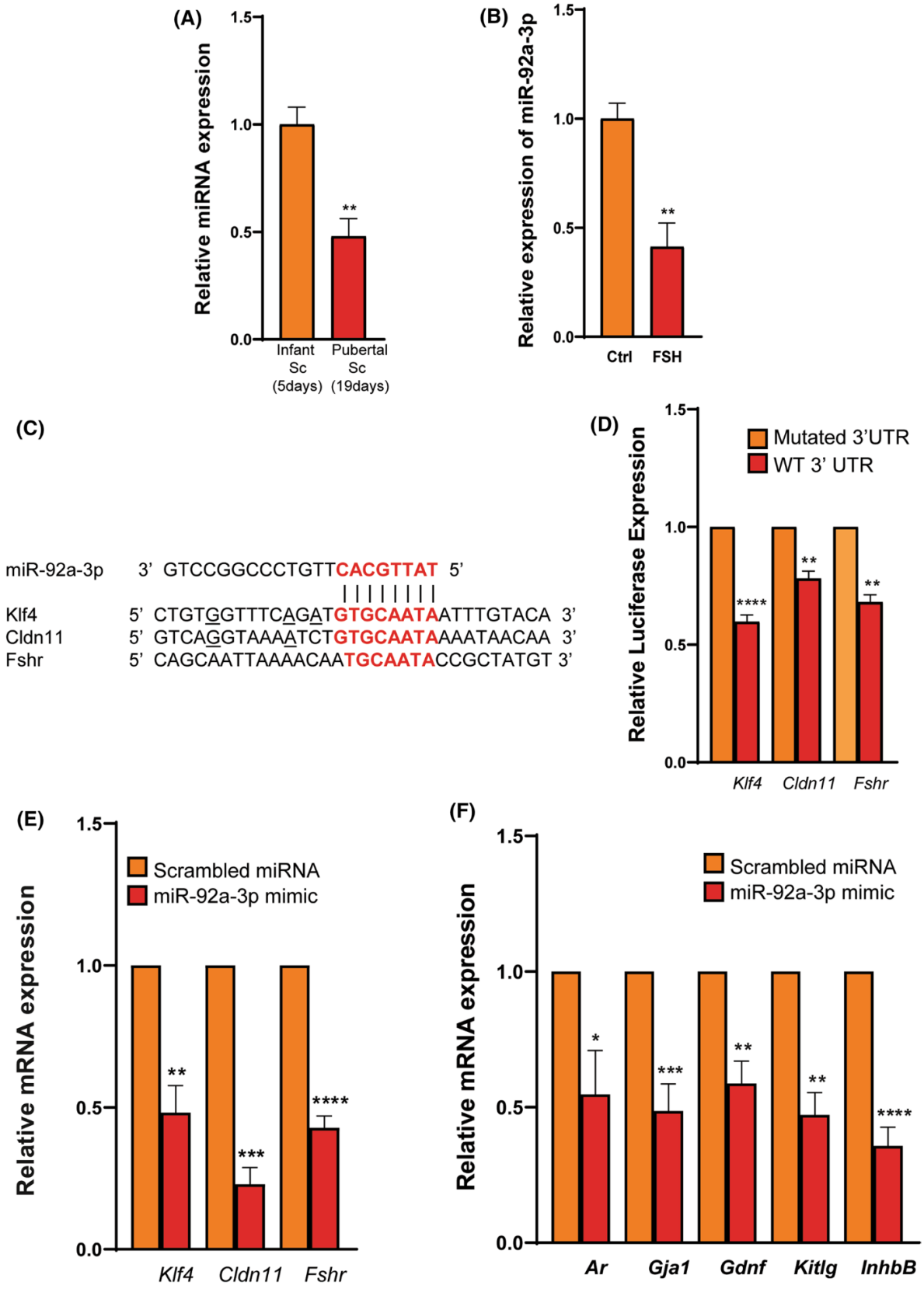
(A)
Relative miRNA expression
1.5
1.0
0.5
0.0
**
Infant Sc (5days)
Pubertal Sc (19days)
(B)
Relative expression of miR-92a-3p
1.5
1.0
0.5
0.0
**
Ctrl
FSH
(C)
miR-92a-3p 3' GTCCGGCCCTGTTCACGTTAT 5'
Klf4 5' CTGTGGTTTCAGATGTGCAATAATTTGTACA 3'
Cldn11 5' GTCAGGTAAAATCTGTGCAATAAAATAACAA 3'
Fshr 5' CAGCAATTAAAACAATGCAATACCGCTATGT 3'
(D)
Relative Luciferase Expression
Mutated 3'UTR
WT 3' UTR
1.5
1.0
0.5
0.0
****
**
**
Klf4
Cldn11
Fshr
(E)
Relative mRNA expression
Scrambled miRNA
miR-92a-3p mimic
1.5
1.0
0.5
0.0
**
***
****
Klf4
Cldn11
Fshr
(F)
Relative mRNA expression
Scrambled miRNA
miR-92a-3p mimic
1.5
1.0
0.5
0.0
*
***
**
**
****
Ar
Gja1
Gdnf
Kitlg
InhbB

◂**Fig. 1** Validation of miR-92a-3p-predicted target genes and effect of miR-92a-3p overexpression in pubertal (19 days old) rat Sc. (**A**) q-RT-PCR data showing the levels of miR-92a-3p in cultured infant (5 days old) and pubertal (19 days old) rat Sc, (**B**) q-RT-PCR data showing the levels of miR-92a-3p in FSH-treated cultured pubertal (19 days old) rat Sc as compared to untreated Sc, (**C**) MiR-92a-3p sequence (3′ to 5') and its binding site on the 3'UTR of the predicted target genes, (**D**) luciferase analysis of WT and mutated 3'UTRs of predicted target genes of miR-92a-3p in HEK293T cells using synthetic Rno-miR-92a-3p mimic, (**E**) mRNA expression for direct targets of miR-92a-3p in cultured pubertal (19 days old) rat Sc as compared to scramble controls, (**F**) q-RT-PCR data showing change in levels of genes involved in Sc functional maturation, in miR-92a-3p mimic transfected cultured rat pubertal (19 days old) Sc as compared to scramble transfected Sc. All values are mean ± SEM of at least three independent biological replicates. Paired Student's *t* test was used for determining statistical significance. $p < 0.05$ was considered to be statistically significant

critical role of miR-92a-3p in FSH-mediated Sc maturation and male fertility.

## Results

### Differential expression of miR-92a-3p in infant (5 days old) and pubertal (19 days old) rat Sc and regulation of its expression in pubertal Sc by FSH

MiR-92a-3p levels were found to be significantly ($p < 0.05$) declined in cultured pubertal (19 days old) rat Sc as compared to cultured infant (5 days old) Sc, both of which were given a pulsatile co-treatment with FSH and testosterone (Fig. 1A). We attempted to understand the regulation of decline in miR-92a-3p expression in pubertal Sc by treating them with FSH. MiR-92a-3p expression levels declined significantly ($p < 0.05$) in response to FSH in cultured pubertal (19 days old) Sc as compared to untreated pubertal Sc (Fig. 1B).

### In vitro validation of genes predicted to be targeted by miR-92a-3p

We performed luciferase assay to validate the targets of miR-92a-3p in HEK293T (human embryonic kidney cells) which were used as host cells for conducting luciferase assay as they are easy to transfect. For validating the predicted targets of miR-92a-3p, we co-transfected synthetic Rno-miR-92a-3p mimic with the WT or mutated 3' UTR (of target genes) bound luciferase in HEK293T cells. Genes like *Klf4, Cldn11* and *Fshr* were found to be directly targeted by miR-92a-3p (Fig. 1C, D). We then sought to validate these direct targets of miR-92a-3p by q-RT-PCR in pubertal (19 days old) Sc transfected with commercial Rno-miR-92a-3p mimics (miRNA overexpression) or scrambled controls. MiR-92a-3p overexpression significantly ($p < 0.05$) downregulated the transcript levels of *Klf4, Cldn11* and *Fshr* in cultured 19-day rat Sc (Fig. 1E). The transcript levels of other reported targets of miR-92a-3p such as *Pten, Rora, Sirt1* and *Esr1*, and predicted targets such as *Lats1* and *Tead1* were also significantly ($p < 0.05$) downregulated in miR-92a-3p mimic-transfected pubertal rat Sc as compared to scrambled miRNA-transfected Sc (Supp. Fig. 1A).

### MiR-92a-3p overexpression in cultured pubertal Sc compromised its functional maturation

The expression of genes such as *Ar, Gja1, Kitlg, Gdnf* and *InhbB,* which are critically essential for spermatogenesis, were significantly ($p < 0.05$) downregulated in miR-92a-3p-overexpressing pubertal rat Sc as compared to scrambled miRNA-transfected Sc (Fig. 1F).

### Generation of transgenic mice with Sc-specific overexpression of miR-92a-3p

Since the in vitro overexpression of miR-92a-3p in pubertal rat Sc resulted in a prominent decline in the expression of functional maturation markers of the cell, we generated a transgenic mouse model overexpressing miR-92a-3p (miR-92a-Tg mice) in Sc. The expression of miRNA was driven under the proximal *Rhox5* promoter, which ensured the overexpression of miR-92a-3p specifically in Sc at the onset of puberty (Supp. Fig. 2A). Slot blot analysis of the F1 generation from the electroporated fore-founder mice identified the transgene-positive animals (Supp. Fig. 2B). MiR-92a-3p levels were significantly ($p < 0.05$) upregulated in the transgenic testes as compared to age-matched wild-type (WT) controls (Fig. 2A). Despite a similar body weight in miR-92a-3p-overexpressing transgenic mice and WT controls, there was a significant ($p < 0.05$) decline in the testis weight of the transgenic mice (Supp. Fig. 2C, D). The testis size (Fig. 2B) was evidently reduced in the miR-92a-3p transgenic mice from F1 generation and F2 generation (Supp. Fig. 2E). The percentage ratio of testis weight to body weight, gonadosomatic index (GSI %) also showed a sharp decline in the miR-92a-3p-overexpressing transgenic mice as compared to age-matched WT mice (Fig. 2C).

### MiR-92a-3p-overexpressing transgenic mice were infertile showing testicular atrophy

The total epididymal sperm count was lower than one million per ml in miR-92a-Tg mice as compared to age-matched WT mice that had an average sperm count of more than 5 million per ml (Fig. 2D). The miR-92a-Tg mice were completely infertile, as they failed to produce any litter despite

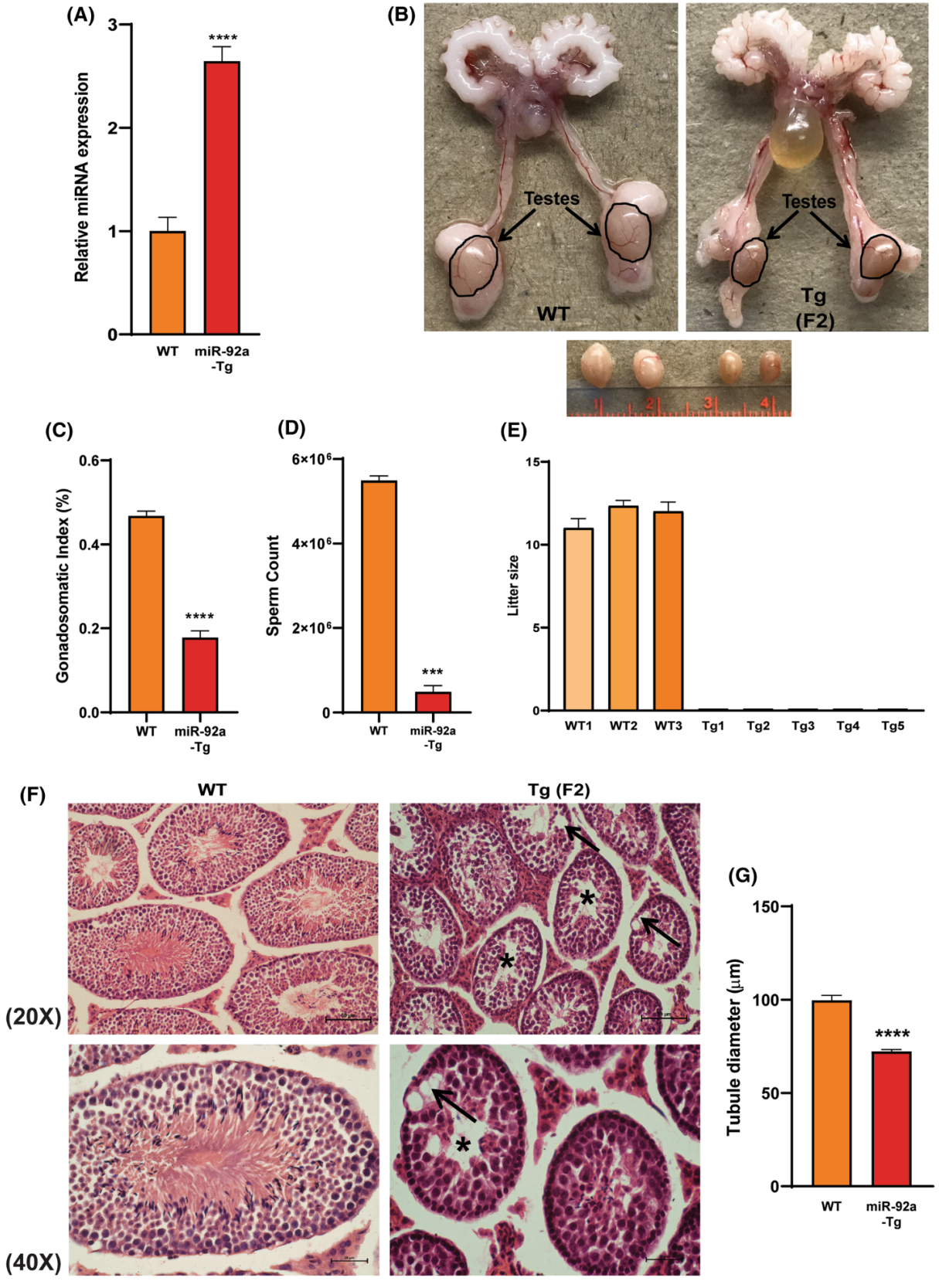
(A)
Relative miRNA expression
3
2
1
0
****
WT
miR-92a -Tg
(B)
Testes
WT
Testes
Tg (F2)
(C)
Gonadosomatic Index (%)
0.6
0.4
0.2
0.0
****
WT
miR-92a -Tg
(D)
Sperm Count
6×10⁶
4×10⁶
2×10⁶
0
***
WT
miR-92a -Tg
(E)
Litter size
15
10
5
0
WT1
WT2
WT3
Tg1
Tg2
Tg3
Tg4
Tg5
(F)
WT
Tg (F2)
(20X)
(40X)
(G)
Tubule diameter (μm)
150
100
50
0
****
WT
miR-92a -Tg

◂**Fig. 2** miR-92a-3p in Sc-overexpressing transgenic mice had reduced testis size and low epididymal sperm count. (**A**) q-RT-PCR data showing the levels of miR-92a-3p in transgenic mice testis as compared to age-matched WT control mice testis. (**B**) Representative image of testis size and seminal vesicles of mir-92a-3p-overexpressing transgenic mice from F2 generation as compared to age-matched WT controls. (**C**) Gonadosomatic index (testis weight/body weight × 100) of WT and transgenic mice overexpressing miR-92a-3p. (**D**) Epididymal sperm count (million per mL) in control and miR-92a-3p-overexpressing transgenic mice. (**E**) Average litter produced by miR-92a-3p transgenic mice as compared to age-matched WT controls. (**F**) Representative images of haematoxylin and eosin staining of testicular paraffin sections from miR-92a-3p transgenic mice from F2 generation and age-matched WT controls. Images captured at 20X (scale bar 50 µm) and 40 X (scale bar 20 µm) objective magnifications. Black arrows point at vacuoles observed towards the basal lamina. Asterisk marks represent tubules with very low numbers of mature sperms. (**G**) Tubule diameter as measured in the testis from miR-92a transgenic and WT mice. At least three different sections from each animal (each with at least 5 seminiferous tubules at 20X magnification) were analysed to measure the tubule diameter. All values are mean ± SEM of at least five WT and five transgenic mice. Unpaired Student's *t* test was used for determining statistical significance. $p < 0.05$ was considered to be statistically significant

successful coitus, whereas the WT mice consistently produced 10–12 pups in each litter (Fig. 2E). This was confirmed by checking the vaginal plugs in the female mice that were mated with either miR-92a-Tg male mice or WT males. In contrast to the WT testis, the seminiferous tubules in the testis of miR-92a-Tg mice from both F1 and F2 generation had significantly ($p < 0.05$) reduced tubule size and discernible histological differences with disrupted seminiferous tubule architecture as observed with haematoxylin and eosin staining on tissue paraffin sections (Fig. 2F, G and Supp. Fig. 2E). The tubules also had a vacuolated phenotype towards the basal lamina in the transgenic mice testis (Fig. 2F).

## MiR-92a-3p overexpression impaired Sc maturation and increased germ cell apoptosis

The testicular mRNA levels of *Klf4, Cldn11* and *Fshr* that are directly targeted by miR-92a-3p were significantly ($p < 0.05$) declined in the transgenic mice as compared to age-matched WT mice (Fig. 3A). The functional maturation markers of Sc such as *Ar, Gja1, Gdnf, Kitlg, Abp* and *InhbB* were also significantly downregulated in miR-92a-Tg mice testis as compared to that of the age-matched WT control animals (Fig. 3B). These results were concordant with the findings obtained in our in vitro experiments with cultured pubertal (19 days old) Sc from rats. To ensure that miR-92a-3p overexpression specifically causes repression of its gene targets, and not a global repression in transcription, we compared the transcript levels of genes that are not predicted to be targeted by miR-92a-3p. The testicular mRNA levels of *Creb1*, *Runx2*, *Pitx2* and *Ctnnb* failed to show any significant changes in their expression (Supp. Fig. 3), thus indicating that overexpression of miR-92a-3p had a direct impact on its target genes and Sc functional maturity markers. The decline in the Sc maturation markers was also associated with an increase in the number of apoptotic Gc. The number of apoptotic cells per tubule as detected by TUNEL assay was significantly ($p < 0.05$) higher in the transgenic mice testis as compared to WT testis (Fig. 3C, D).

## MiR-92a-3p-overexpressing transgenic mice exhibited low number of mitotically active Gc and an increased number of Sc

We intended to detect any proliferation of Sc in adult miR-92a-Tg mice, which in turn would explain the maturational status of Sc in transgenic mice that fail to undergo timely maturation. To this end, we performed co-immunostaining for proliferating cell nuclear antigen (PCNA) and Sc-specific SOX9 on tissue sections from adult transgenic and age-matched WT mice (Fig. 4A). The total number of PCNA-positive mitotically active cells per tubule was significantly reduced, while SOX9-positive Sertoli cells per tubule were significantly ($p < 0.05$) higher in the transgenic mice as compared to age-matched WT controls (Fig. 4B, C). Interestingly, there were no double-positive (PCNA and SOX9) Sc (Fig. 4A), indicating that adult Sc in Tg mice were not proliferative in nature and that there was a significantly ($p < 0.05$) lesser number of mitotically active Gc in the Tg mice. In addition to this, there was a significant ($p < 0.05$) increase in the testicular transcript levels of *Sox9* in the miR-92a-Tg mice as compared to age-matched WT control mice (Fig. 4D).

## MiR-92a-3p overexpression in transgenic mice led to disruption of the blood– testis barrier (BTB)

Since the testicular mRNA levels of *Cldn11* (*claudin11*) and *Gja1* (*connexin43*) were found to be reduced in miR-92a-Tg mice as compared to age-matched WT mice (as shown in Fig. 3A, B), we further investigated the protein level expression of these BTB components. Immunohistochemistry for claudin11 and connexin43 on frozen testicular sections (7 µm) showed that the transgenic mice testis expressed very low levels of these proteins as compared to age-matched WT testis (Fig. 5A–D). Moreover, testicular protein level of Cx43 (encoded by *Gja1*) was also found to be significantly reduced in immunoblot analysis (Supp. Fig. 4). Transmission electron microscopy (TEM) of freshly collected testis from miR-92a-Tg and age-matched WT mice revealed a discontinuous and relatively narrow BTB in the

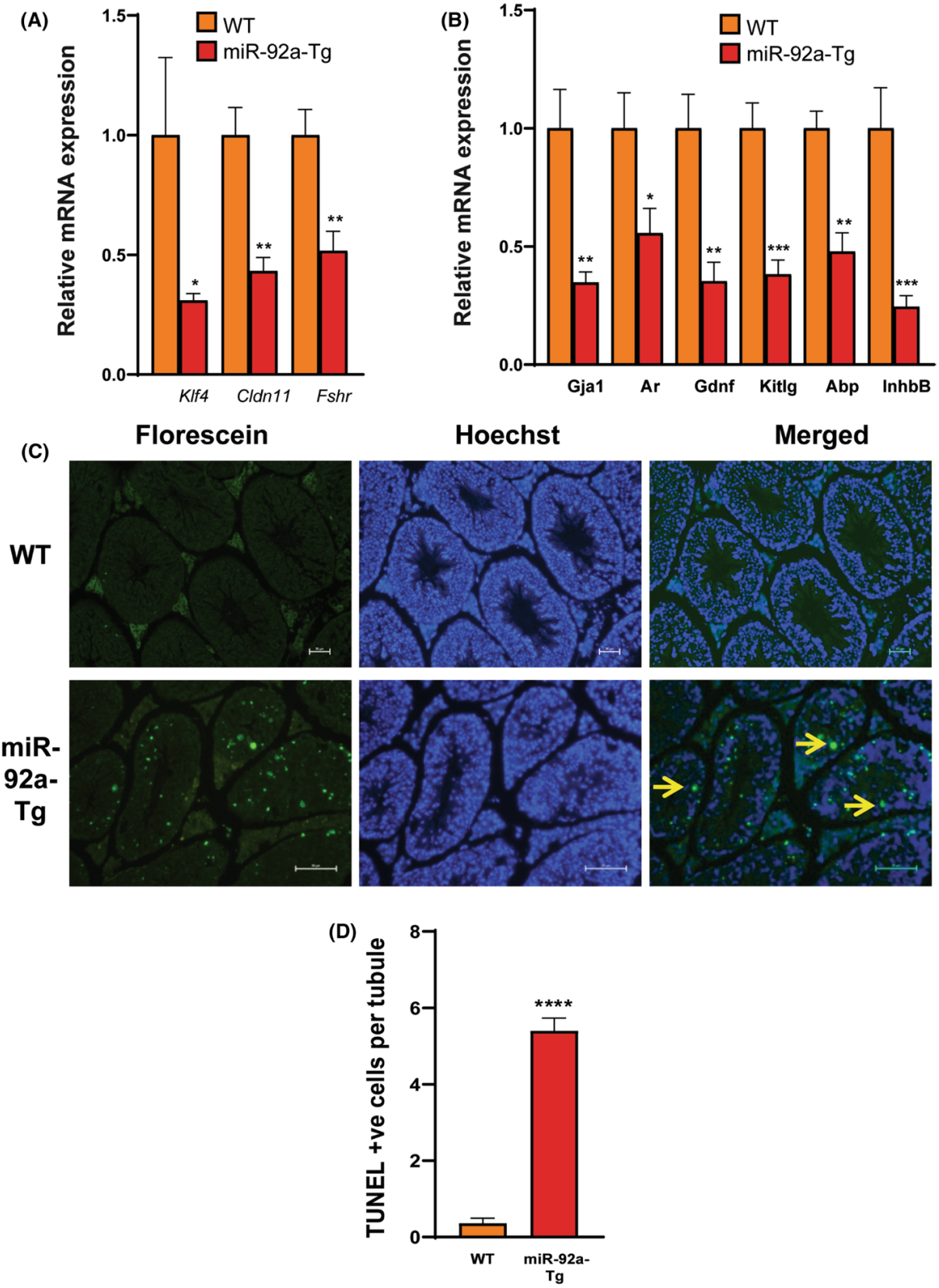
(A)
Relative mRNA expression
1.5
1.0
0.5
0.0
WT
miR-92a-Tg
*
**
**
Klf4
Cldn11
Fshr
(B)
Relative mRNA expression
1.5
1.0
0.5
0.0
WT
miR-92a-Tg
**
*
**
***
**
***
Gja1
Ar
Gdnf
Kitlg
Abp
InhbB
(C)
Florescein
Hoechst
Merged
WT
miR-92a-Tg
(D)
TUNEL +ve cells per tubule
8
6
4
2
0
****
WT
miR-92a-Tg

◂**Fig. 3** miR-92a-3p overexpression in transgenic mice impaired Sc maturity and was associated with germ cell apoptosis. (**A**) mRNA expression data showing levels of genes directly targeted by miR-92a-3p in miR-92a-Tg mice testis as compared to age-matched WT mice testis. (**B**) mRNA expression data showing the levels of Sc functional maturation marker genes in miR-92a-Tg mice testis as compared to age-matched WT mice testis. (**C**) Representative image of testicular sections (7 µm) of miR-92a-3p transgenic and WT mice showing apoptotic germ cells as detected by TUNEL assay. Arrows indicate TUNEL-positive cells. Images captured at 20X (scale bar 50 µm) objective magnification, (**D**) Quantification of TUNEL-positive cells per tubule in transgenic mice testis as compared to WT testis. At least three different sections from each animal (each with at least 10 seminiferous tubules at 10X magnification) were analysed to determine the extent of germ cell apoptosis. Nuclei were stained with Hoechst. All values are mean ± SEM of at least five WT and five transgenic mice. Unpaired Student's *t* test was used for determining statistical significance. $p < 0.05$ was considered to be statistically significant

Tg mice as compared to the intact BTB in age-matched WT controls (Fig. 5E).

## Discussion

FSH signalling via testicular Sc plays a critical role in spermatogenesis [13, 44]. FSH acts as a mitogen in foetal and neonatal Sc and such proliferation of Sc ceases during pubertal testicular development setting the upper limit of spermatogenic output of the adult testes [16, 45–48]. A developmental shift in FSH signalling has been observed in maturing rat Sc with an enhanced FSH binding to FSHR, leading to the rapid transition of spermatogonia A to B [18]. MicroRNAs are critical *trans-acting* factors regulating developmental gene expression during testicular differentiation [37, 49–51]. Both FSH and T induce a series of miRNAs to regulate the transcriptome of Sc [52–54]. We have found in the past that expression of miR-92a-3p declines at puberty and in the present study we have deciphered its role on male fertility [41].

We overexpressed miR-92a-3p in pubertal Sc in vitro, using commercial miRNA mimics. The validated direct targets of miR-92a-3p included genes such as *Fshr, Klf4, Cldn11, Lats1* and *Tead1*. Additionally, previously reported targets of miR-92a-3p such as *Pten, Rora, Sirt1* and *Esr1* were also validated in pubertal Sc, as positive controls [55–61]. Our in vitro data showed that overexpression of miR-92a-3p in pubertal Sc led to significant decline in critical FSH-responsive genes such as *Ar, Gja1, Kitlg, Gdnf* and *InhbB*, which are known to nurture Gc division and differentiation to support spermatogenesis. For example, Kit ligand (coded by *Kitlg*) or stem cell factor (SCF) and glial cell-derived neurotropic factor (coded by *Gdnf*) are reported to be essential for renewal of SSC, whereas claudin11 (coded by *Cldn11*) or connexin43 (coded by *Gja1*) are the major Sc–Sc and Sc–Gc junctional proteins that are essential components of the BTB [62–65]. Reduced expression of these genes is often associated with azoospermia or oligozoospermia.

Intriguingly, FSH also significantly downregulated the levels of miR-92a-3p in cultured pubertal rat Sc. This led us to investigate the probable role of FSH-responsive miR-92a-3p in Sc maturation and functionality. We therefore prevented the natural decline of miR-92a-3p in pubertal testes by generating a novel transgenic mouse model (miR-92a-Tg). The uninterrupted overexpression of miR-92a-3p in pubertal and post-pubertal transgenic mice was achieved by driving the expression of pri-miR-92a-3p under proximal *Rhox5* (Pem) promoter, which gets activated in Sc at around 14 days of post-natal age and continues to express the tagged gene during adulthood in all stages of seminiferous cycles, in particular stages VI–VIII in an FSH-independent manner [66–68]. The *Rhox5* promoter is reported to be expressed in the epididymis [69]. However, changes in epididymal miRNA levels would not affect the testicular architecture, which was critically damaged in the miR-92a-Tg mice. The histological analysis of testicular sections from the transgenic mice revealed the presence of few sperms in some tubules. This indicated that the defects in fertility due to overexpression of miR-92a-3p originated within the testes. Overexpression of miR-92a-3p in the transgenic mice resulted in severe dysregulation of the Sc functional maturation, compromising its ability to support Gc division and differentiation, thereby leading to a significant reduction in the testis size, with acute oligozoospermia and complete infertility in these mice. The Lc function in adult transgenic testes was, however, not affected due to overexpression of miR-92a-3p. This was evident from the size of the seminal vesicles, which were similar in transgenic and age-matched WT control mice. The distorted testicular architecture of the miR-92a-Tg mice also lead to massive Gc apoptosis.

Furthermore, a significant decline in the number of mitotically active Gc was found in the transgenic testes as compared to age-matched WT controls, indicating that mostly pre-meiotic Gc (mitotic Gc) were undergoing apoptosis. Although there has been a significant increase in the Sc number (as evidenced by an increased number of SOX9 immunopositive cells) in adult miR-92a-Tg testes, Sc were mitotically inactive. This can be justified, as PCNA-positive cells fail to overlap with the SOX9-positive cells in adult miR-92a-Tg testes. Our data indicated that the number of mitotic Gc were significantly low in adult transgenic testes, corroborating with the reduced epididymal sperm count. Furthermore, our data showed a delayed pubertal onset of Sc maturation in miR-92a-Tg mice, with poor expression of *Ar*, *Klf4*, *Cldn11*, *Gja1*, *Kitlg, Gdnf* and *InhbB* transcripts, thereby having compromised functionality to support robust Gc division and development. FSH and T play critical role in functional maturation of Sc during puberty, which is a

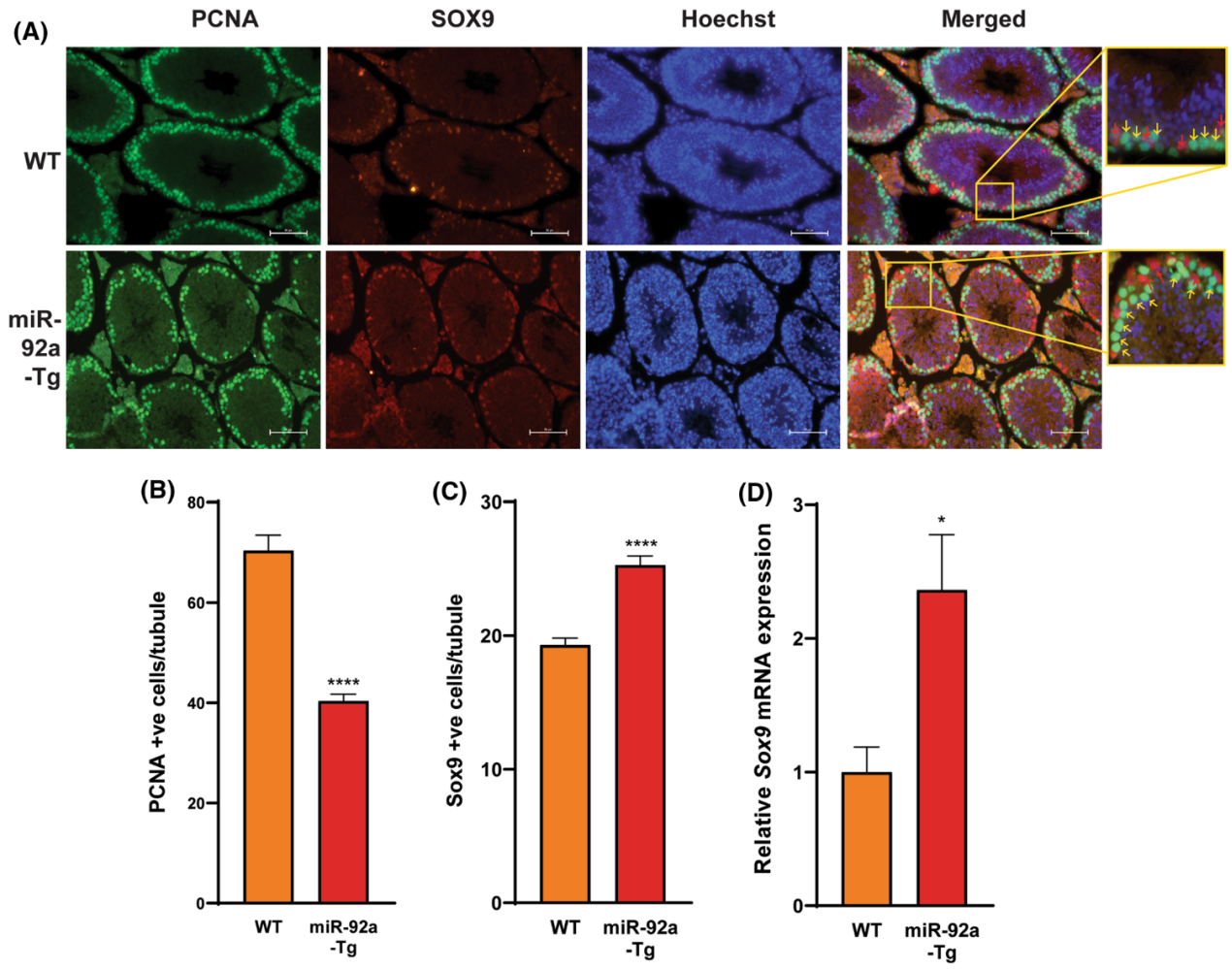


**Fig. 4** miR-92a-3p transgenic mice had an increased number of Sc. (**A**) Representative image of co-immunostaining for PCNA and Sc-specific SOX9 on testis paraffin section (7 µm) from transgenic and WT mice. Nuclei were stained with Hoechst. Images captured at 20X (scale bar 50 µm) objective magnifications. Inset shows magnified image of a part of the tubule. Yellow arrows indicate PCNA-positive cells and red arrow indicates SOX9-positive cells, (**B**) Quantification of PCNA-positive cells per tubule in transgenic mice testis as compared to WT testis, (**C**) Quantification of SOX9-positive cells per tubule in transgenic mice testis as compared to WT testis. At least three different sections from each animal (each with at least 10 seminiferous tubules at 10X magnification) were analysed to count the number of PCNA/SOX9-positive cells. Nuclei were stained with Hoechst, (**D**) Testicular mRNA levels of *Sox9* in miR-92a-Tg mice as compared to age-matched WT testis. All values are mean ± SEM of at least five WT and five transgenic mice. Unpaired Student's *t* test was used for determining statistical significance. $p < 0.05$ was considered to be statistically significant

prerequisite for establishing male fertility [70, 71]. Persistent presence of immature Sc in adult testes has been reported to be associated with male infertility in human and rodent models [24, 41, 67, 72–76]. It is essential to note here that despite such rise in Sc number in adult transgenic testes, *Fshr* mRNA expression in whole testicular extract was found to be significantly low in miR-92a-Tg mice probably due to a substantial decline in FSHR in individual Sc, suggesting poor FSH signalling in adult transgenic testes.

Our results demonstrated that preventing the natural decline of miR-92a-3p levels in the mice testis severely affected BTB formation. Besides T, FSH has also been shown to directly upregulate these junction molecules in primary Sc culture [77, 78]. Poor expression of these junction proteins was further justified by low level of *Fshr* and *Ar* found in the adult miR-92a-Tg mice as compared to WT controls. The expression of AR is induced by FSH in Sc [79–81]. The AR-responsive tight junction protein Claudin11 and gap junction protein Connexin43 are the major components of the BTB, which spatially protects the neoantigens, expressed during the development of new Gc from the reach of immune surveillance [15]. Consistent with the

immunohistological data of claudin11 or connexin43, the ultra-architecture of BTB was found to be discontinuous and non-uniform in the transgenic testis as evidenced by TEM imaging. The disruption of BTB is known to cause male infertility as reported in Sc-specific ablation of *Cldn11* or *Gja1,* where the polarity of Sc gets impaired leading to delayed and disturbed functional maturation of Sc [82, 83]. The disruption of the BTB may be responsible for the severe oligozoospermia observed in the miR-92a-3p-overexpressing transgenic mice.

Kruppel-like factor 4 (KLF4) is a pleiotropic zinc finger transcription factor that critically regulates cellular differentiation and cell cycle control and has been previously reported to be directly targeted by miR-92a-3p [84–88]. Our miR-92a-Tg mice showed significant decline in *Klf4* transcript level in adult testes as compared to age-matched WT mice. KLF4 is known to be highly responsive to FSH and we found similar upregulated expression of *Klf4* by FSH in normal pubertal rat Sc. Sc-specific selective ablation of *Klf4* in mice has been shown to affect the terminal differentiation of Sc, leading to compromised vesicular transport and secretory capacity of these cells [85, 87, 89]. MiR-92a-3p-mediated downregulation of KLF4 might have played a crucial role in limiting Sc maturation.

In summary, we for the first time have demonstrated a critical role of miR-92a-3p, in regulating Sc function and male fertility. Our results suggested that preventing the natural decline of miR-92a-3p in pubertal Sc by its uninterrupted presence in post-pubertal cells leads to a compromised maturation and functioning of Sc, disruption of the BTB and Gc apoptosis, resulting in acute oligozoospermia and complete male infertility. These findings can be attributed to reduced expression of genes such as *Fshr*, *Cldn11* and *Klf4,* which are directly targeted by miR-92a-3p and genes such as *AR*, *Gdnf*, *Kitlg*, *Gja1* and *Inhbb*, which are critical for Sc functions. We therefore infer that the FSH-induced pubertal decline in miR-92a-3p is critical for the adequate FSH signalling to occur at puberty, which in turn is necessary for the timely maturation of Sc and subsequent spermatogenic onset. However, more detailed studies are required to reveal the regulatory network of miR-92a-3p and its impact on FSH-induced transcriptome in Sc. This study showed that deregulated expression of miR-92a-3p due to genetic or lifestyle factors may be one of the important aetiologies for some forms of idiopathic male infertility. Our data can be helpful to diagnose such cases appropriately using miR-92a-3p as a potential marker of fertility and such individuals can be cured by manipulating the expression of miR-92a-3p in the testis using transient transfections with viral vectors or in cultures using testicular biopsies.

## Conclusion

This study has established the role of miR-92a-3p in maturation of Sc and male fertility by directly targeting genes such as *Klf4*, *Cldn11* and *Fshr*. Our observations suggested that the FSH-induced downregulation of miR-92a-3p in Sc is critical for pubertal onset of robust Gc differentiation at the onset of puberty. Persistent expression of this microRNA in adult transgenic testes resulted in compromised maturation of Sc and impaired spermatogenic progression. Sc-specific overexpression of miR-92a-Tg mice was associated with disruption of BTB and massive Gc death resulting in infertility. Therefore, it is reasonable to conclude that the sustained expression of miR-92a-3p in adult testes may be a putative cause of idiopathic male infertility, and manipulation of miR-92a-3p expression ex vivo or in vivo may serve as potential therapy for treatment of infertility/sub-fertility.

## Materials and methods

### Animals and reagents used

Wistar rats and FVB/J mice used in this study were procured from the Small Animal Facility of the National Institute of Immunology, New Delhi, India. All animals were housed and used as per the guidelines laid down by the Committee for the Purpose of Control and Supervision of the Experiments on Animals (CPCSEA). All animal-related experimental protocols followed were approved by the Institutional Animal Ethics Committee (IAEC). All reagents were purchased from Sigma (St. Louis, USA) unless stated otherwise.

### Cell culture

#### Rat Sertoli cell culture

Testes were obtained from 20 to 22 infant (5 days old) and 5–6 pubertal (19 days old) Wistar rats for Sc isolation and culture as described previously [18, 90]. Briefly, the animals were euthanized by $CO_2$ asphyxiation and the testes were dissected out and decapsulated using fine forceps to unpack the seminiferous tubules which were then chopped with a sterile scalpel. These finely chopped tubules were subjected to sequential enzymatic digestion with collagenase (3 mg/20 ml, for 30–35 min) and pancreatin (3 mg/20 ml, for ~ 2 min). This ensured the removal of other testicular cells, namely interstitial cells and peritubular myoid cells, respectively. The cells so obtained were plated in 12-well cell culture plates at a density of $8–9 \times 10^5$ cells/clusters per well in DMEM/HAM's F-12 media with 1% fetal bovine serum (FBS) and kept in a humidified cell culture incubator

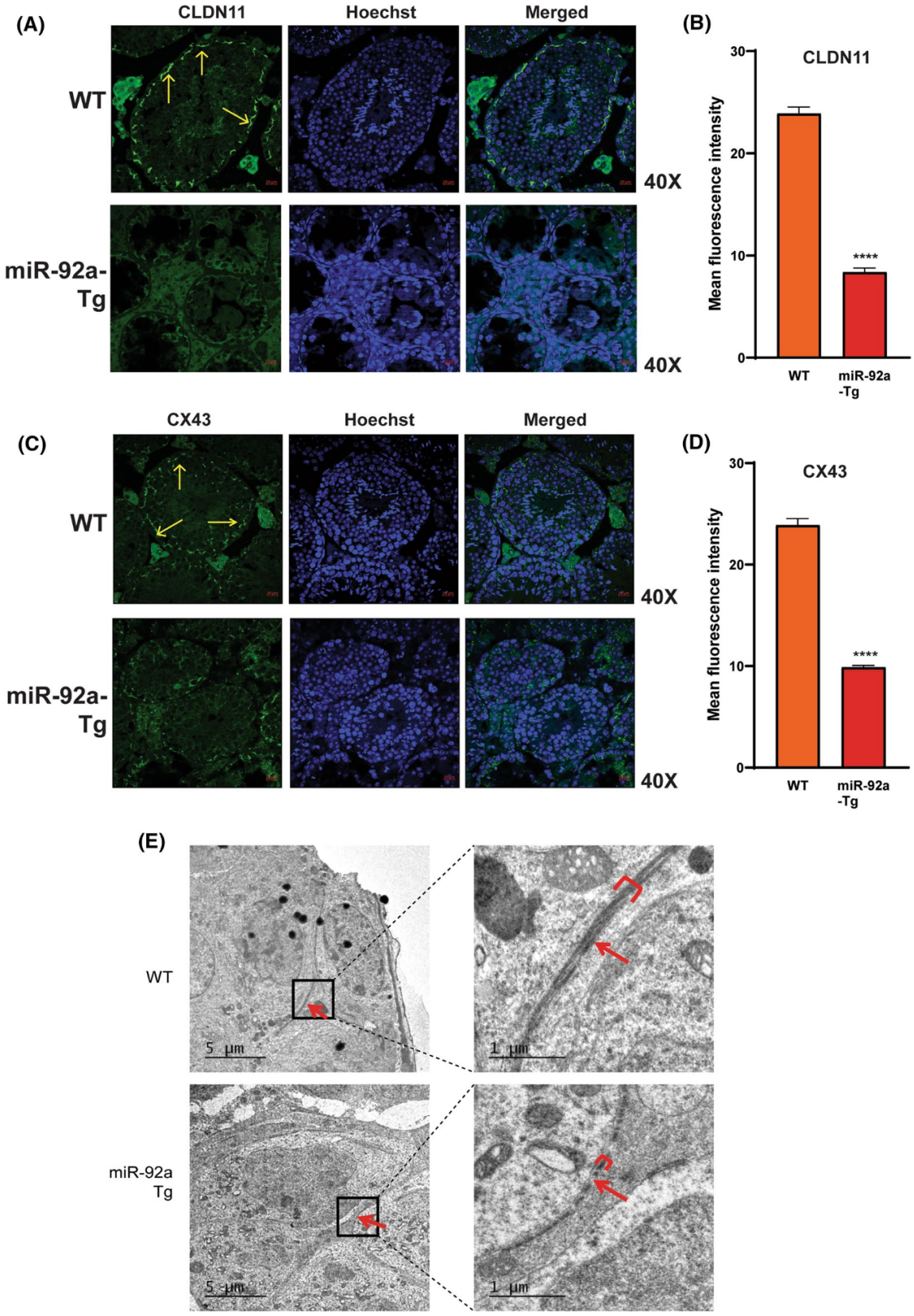
(A)
CLDN11
Hoechst
Merged
WT
40X
miR-92a-Tg
40X
(B)
CLDN11
Mean fluorescence intensity
30
20
10
0
****
WT
miR-92a -Tg
(C)
CX43
Hoechst
Merged
WT
40X
miR-92a-Tg
40X
(D)
CX43
Mean fluorescence intensity
30
20
10
0
****
WT
miR-92a -Tg
(E)
WT
5 µm
1 µm
miR-92a Tg
5 µm
1 µm

◂**Fig. 5** miR-92a-3p overexpression in transgenic mice led to a defective BTB. (**A**) Representative image of immunostaining for claudin11 on testis frozen sections (7 µm) from miR-92a-3p-overexpressing transgenic mice and WT mice. Nuclei were stained with Hoechst. Arrows indicate expression of claudin11. Images captured at 40X (scale bar 20 µm) objective magnifications, (**B**) Quantification of mean fluorescence intensity per tubule in WT and miR-92a-Tg immuno-stained tissue sections, (**C**) Representative image of immunostaining for connexin43 (coded by *Gja1*) on testis frozen sections (7 µm) from transgenic mice and age-matched WT mice. Nuclei were stained with Hoechst. Arrows indicate expression of connexin43. Images captured at 40X (scale bar 20 µm) objective magnifications, (**D**) Quantification of mean fluorescence intensity per tubule in WT and miR-92a-Tg immunostained tissue sections, (**E**) TEM images from transgenic mice testis and WT testis showing the BTB near the Sc nucleus (marked with red arrows and braces, scale bar of 5 µm). Higher magnification (scale bar of 1 µm) of marked area to show discontinuous BTB in transgenic testis as compared to an intact continuous BTB in WT controls

maintained at 34 °C with 5% $CO_2$. After 24 h, cells were replenished with fresh serum-free media supplemented with 1% growth factor (5 µg/ml sodium selenite, 10 µg/ml insulin, 5 µg/ml transferrin, and 2.5 ng/ml epidermal growth factor). On the third day, cells were subjected to a brief hypotonic shock using 20 mM Tris–HCl dissolved in culture media, to remove any contaminating germ cells. The cells were subjected to various treatments on day 4 of culture. Sc culture purity was assessed by SOX9 immunostaining along with Hoechst (Supp. Fig. 4).

#### HEK-293 T cell culture

HEK cells were cultured in DMEM high glucose media supplemented with 10% FBS and maintained in humidified cell culture incubator at 37 °C with 5% $CO_2$. All experiments were performed at the third or fourth passage of culture, at a seeding density of $0.05 \times 10^6$ in 24-well cell culture plates and transfected at ~ 70% cell confluency.

## Plasmid cloning

#### Cloning of UTRs in PmirGlo

The 3′ UTRs of the predicted targets of miRNA-92a-3p were obtained from the MiRDB database (mirdb.com). The miRNA binding site on the 3′ UTR along with its flanking sequences (25 bp each) was taken from the MiRDB database. This sequence was then synthesized as a pair of complementary single-stranded DNA oligos (Sigma Aldrich). The 3′ UTRs were mutated for use as control plasmids, where the seed sequence binding region was replaced by Ts. All oligos were designed such that upon annealing, they generated overhangs compatible with those generated by NheI (3′) and SalI (5′) digestion. The oligos were annealed and the product was checked on 4% agarose gel to ensure the annealing efficiency. The annealed insert was then ligated to the PmirGlo Dual Luciferase plasmid digested with the same set of restriction enzymes (NheI and SalI). To assist the screening of the bacterial colony harbouring the desired clone, a unique restriction enzyme site (EcoRI) was introduced at the 3′ end of the UTR sequences during its design. The ligated product was transformed into *E.coli* DH5α competent cells and positive clones were identified by double digesting the isolated plasmid samples with EcoRI and HindIII. The plasmid was then used for transfecting HEK cells. The list of UTRs cloned has been provided in Table 1.

#### Cloning of miR-92a-3p overexpression plasmid in dual PEM (Rhox5) vector

The primary microRNA (pri-miRNA) sequence for Mmu-miR-92a was obtained from the miRBase database (www.mirbase.com). The pri-miRNA sequence and the upstream/downstream 200 bp flanking sequences were PCR amplified from mouse genomic DNA. The forward and reverse primers were designed to have EcoRI and SalI restriction sites, respectively, to facilitate its cloning in dual PEM (Rhox5) plasmid vector double digested with the same set of enzymes. The dual PEM vector was designed on an IRES backbone. The insert was cloned downstream of the first PEM promoter which drives the expression of the gene of interest, while the second PEM promoter drives the expression of the GFP reporter gene. The vector and insert were ligated and transformed into *E.coli*. The colonies obtained were screened by colony PCR with specific primers on the vector backbone and the insert.

## In vitro treatments

#### Pulsatile hormone treatment of rat Sc

The cultured rat Sc were subjected to hormone treatment on day 4 of the culture in a pulsatile manner [91]. The cells were treated together with ovine follicle-stimulating hormone (50 ng/ml o-FSH) and testosterone ($10^{-7}$ M) for 30 min, followed by 2.5 h incubation with hormone-free media for four cycles. The cells were harvested in TRI reagent at the end of the fourth cycle for RNA isolation.

#### Mimic transfection in rat Sc

On day 4, cultured pubertal (19 days old) Sc were transfected in a 12-well plate with Rno-miR-92a-3p mimic (200 pmol) procured from Dharmacon, using Lipofectamine 2000 (Invitrogen) as per the manufacturer's protocol. Scrambled mimic was used as a negative control. Briefly, the miRNA mimic and Lipofectamine were separately diluted (quick vortex) in 50 µL of Opti-MEM media and mixed together

**Table 1** List of UTRs used for microRNA target validation by luciferase assay

| Name | Sequence |
|---|---|
| KLF4-UTR-WT-FP | CTAGCTAGAATTCTATGCACTGTGGTTTCAGATGTGCAATAATTTGTACAATGGTTTAG |
| KLF4-UTR-WT-RP | TCGACTAAACCATTGTACAAATTATTGCACATCTGAAACCACAGTGCATAGAATTCTAG |
| KLF4-UTR-MUT-FP | CTAGCTAGAATTCTATGCATTTTTTTTTTTTTTTTTTTTATTTGTACAATGGTTTAG |
| KLF4-UTR-MUT-RP | TCGACTAAACCATTGTACAAATAAAAAAAAAAAAAAAAAAAAATGCATAGAATTCTAG |
| CLDN11-UTR-WT-FP | CTAGCTAGAATTCTTGTTCAGGTAAAATCTGTGCAATAAAATAACAAACTGTCTCCAAAGCG |
| CLDN11-UTR-WT-RP | TCGACGCTTTGGAGACAGTTTGTTATTTTATTGCACAGATTTTACCTGAACAAGAATTCTA |
| CLDN11-UTR-MUT-FP | CTAGCTAGAATTCTTGTTTTTTTTTTTTTTTTTTTTTTAAATAACAAACTGTCTCCAAAGCG |
| CLDN11-UTR-MUT-RP | TCGACGCTTTGGAGACAGTTTGTTATTTAAAAAAAAAAAAAAAAAAAAACAAGAATTCTAG |
| FSHR-WT-FP | CTAGCTAGAATTCCTGAATTATTGGTAACAGCAATTAAAACAATGCAATACCGCTATGTGTTTGG |
| FSHR-WT-RP | TCGACCAAACACATAGCGGTATTGCATTGTTTTAATTGCTGTTACCAATAATTCAGGAATTCTAG |
| FSHR-MUT-FP | CTAGCTAGAATTCGCTATAACATGTTTTTTTTTTTTTTTTTTTTACTTTGTTTAAACTACTAAAG |
| FSHR-MUT-RP | TCGACTTTAGTAGTTTAAACAAAGTAAAAAAAAAAAAAAAAAAAACATGTTATAGCGAATTCTAG |
| LATS1-UTR-WT-FP | CTAGCTAGAATTCTAGTGGTTTTACACCTGGATTACTGTGCAATACAGGAGAAAACCAGCTTTGG |
| LATS1-UTR-WT-RP | TCGACCAAAGCTGGTTTTCTCCTGTATTGCACAGTAATCCAGGTGTAAAACCACTAGAATTCTAG |
| LATS1-UTR-MUT-FP | CTAGCTAGAATTCTAGTGGTTTTATTTTTTTTTTTTTTTTTTTTCAGGAGAAAACCAGCTTTGG |
| LATS1-UTR-MUT-RP | TCGACCAAAGCTGGTTTTCTCCTGAAAAAAAAAAAAAAAAAAAAATAAAACCACTAGAATTCTAG |
| TEAD1-UTR-WT-FP | CTAGCTAGAATTCTAACTTTAATACCCATGACAGTTAAGTGCAATTATTTCATCACTCTAAAAG |
| TEAD1-UTR-WT-RP | TCGACTTTTAGAGTGATGAAATAATTGCACTTAACTGTCATGGGTATTAAAGTTAGAATTCTAG |
| TEAD1-UTR-MUT-FP | CTAGCTAGAATTCTAACTTTAATATTTTTTTTTTTTTTTTTTTTATTTCATCACTCTAAAAG |
| TEAD1-UTR-MUT-RP | TCGACTTTTAGAGTGATGAAATAAAAAAAAAAAAAAAAAAAAATATTAAAGTTAGAATTCTAG |
| PTEN-WT-FP | CTAGCTAGAATTCGTTTAGTTTTAGAAAATTTGTGCAATATGTTCATAACGATGGCTGTGGTTG |
| PTEN-WT-RP | TCGACAACCACAGCCATCGTTATGAACATATTGCACAAATTTTCTAAAACTAAACGAATTCTAG |
| PTEN-MUT-FP | CTAGCTAGAATTCGTTTAGTTTTTTTTTTTTTTTTTTTTTGTTCATAACGATGGCTGTGGTTG |
| PTEN-MUT-RP | TCGACAACCACAGCCATCGTTATGAACAAAAAAAAAAAAAAAAAAAAACTAAACGAATTCTAG |
| SIRT1-WT-FP | CTAGCTAGAATTCAGTTGTGAGCTTAAGTGAAGTCTGTGCAATTGCCTGAAGTCCTGTTTCACG |
| SIRT1-WT-RP | TCGACGTGAAACAGGACTTCAGGCAATTGCACAGACTTCACTTAAGCTCACAACTGAATTCTAG |
| SIRT1-MUT-FP | CTAGCTAGAATTCAGTTGTGAGCTTTTTTTTTTTTTTTTTTTTTGCCTGAAGTCCTGTTTCACG |
| SIRT1-MUT-RP | TCGACGTGAAACAGGACTTCAGGCAAAAAAAAAAAAAAAAAAAAAGCTCACAACTGAATTCTAG |
| ESR1-WT-FP | CTAGCTAGAATTCCAAGAACCACAAATGGAAAGTGGATGTGCAATAAGTATTTTGTATGAAAAG |
| ESR1-WT-RP | TCGACTTTTCATACAAAATACTTATTGCACATCCACTTTCCATTTGTGGTTCTTGGAATTCTAG |
| ESR1-MUT-FP | CTAGCTAGAATTCCAAGAACCACAAATTTTTTTTTTTTTTTTTTTTAGTATTTTGTATGAAAAG |
| ESR1-MUT-RP | TCGACTTTTCATACAAAATACTAAAAAAAAAAAAAAAAAAAAATTTGTGGTTCTTGGAATTCTAG |
| RORA-WT-FP | CTAGCTAGAATTCTCTTTTTAATTCTTACCTAGTGCAATATCTGTACATAGAGCACTTGCGGGG |
| RORA-WT-RP | TCGACCCCGCAAGTGCTCTATGTACAGATATTGCACTAGGTAAGAATTAAAAAGAGAATTCTAG |
| RORA-MUT-FP | CTAGCTAGAATTCTCTTTTTTTTTTTTTTTTTTTTTTTTTTCTGTACATAGAGCACTTGCGGGG |
| RORA-MUT-RP | TCGACCCCGCAAGTGCTCTATGTACAGAAAAAAAAAAAAAAAAAAAAAAAAAGAGAATTCTAG |

upon 5 min of incubation at room temperature (RT) to make the transfection mixture. This mixture was incubated further for 20–30 min at RT. Meanwhile, the Sc were drained of its existing media and gently washed once with 1× phosphate-buffered saline (PBS) and kept in 150 µLOpti-MEM (Invitrogen) media and the transfection mixture was added dropwise to the Sc. The cells were then incubated at 34 °C for 9 h, after which the media was changed back to DMEM/Ham's F-12 (with 1% growth factors). The cells were finally harvested in TRI reagent or as cell pellets 24 h post-media change for RNA and protein isolation, respectively.

#### Plasmid transfection in HEK-293 T

HEK293T cells were cultured and at ~ 70% confluency the cells were co-transfected with Rnu-miR-92a-3p mimic (20 pmol) and PmirGlo Dual Luciferase plasmid containing wild-type (WT) or mutated 3'UTR of the target gene (500 ng), using Lipofectamine 2000 (Invitrogen) as per the manufacturer's protocol. Briefly, the mimic and the plasmid were mixed in Opti-MEM and incubated to make the transfection mixture. The existing media of the cells were replaced with the transfection mixture and incubated for 6 h, after which the media were changed back to complete media

(DMEM high Glucose + 10% FBS). The cells were harvested at 24 h post-media change and the cell pellet was stored at − 20 °C for luciferase assay.

## RNA isolation and c-DNA preparation

Total RNA was isolated from Sc frozen in TRI reagent (Sigma Aldrich) using chloroform as described previously [92]. Additionally, sodium acetate (0.3 M) and glycogen (0.2 mg/ml) were added for enhanced precipitation of small RNAs. The quantity and quality (260/280) of RNA were determined using Nanodrop 2000c spectrophotometer (Thermo scientific, USA). 1 µg of RNA was treated with 0.5U DNaseI (ThermoScientific, USA) to remove any contaminating genomic DNA fragments. This was followed by single-strand c-DNA synthesis using M-MLV Reverse Transcriptase (Promega, USA,) as per the manufacturer's protocol.

For the c-DNA synthesis of microRNAs, 1 µg RNA was treated with *E.coli* PolyA Polymerase (NEB) to generate a poly(A)-tail, followed by reverse transcription using 0.5 mg/ml oligo-dT and M-MLV RT. A 32 bp unique sequence was added to the 5' end of the oligo-dT (GCGAGCACA GAATTAATACGACTCACTATAGGTTTTTTTTTTTT), which served as a template for a universal reverse primer for the downstream qPCR analysis of all the miRNA. The entire microRNA sequence was used as the forward primer. Universal reverse primer sequence has been mentioned in Table 2.

## Quantitative real-time PCR

Q-RT PCR was performed in Realplex$^4$ master cycler (Eppendorf, Germany) using Kapa Sybr mix as per the manufacturer's protocol. 1 µL of the c-DNA preparation was taken for each reaction along with 5 µL Kapa Sybr, 0.5 µM each primer (forward and reverse) and 3 µL nuclease-free water (NFW). Melting curve was analysed to detect single amplification peak and the differential expression of gene or miRNA in terms of fold change was calculated using the $2^{(-\Delta\Delta Ct)}$ method as described previously [93]. Each reaction was set in three technical replicates and at least four biological replicates. The expression level of 18S rRNA and let-7a was used for normalizing genes and miRNA expression level, respectively [94]. The list of primers used in the study has been provided in Table 2.

## Luciferase assay for target validation

The harvested HEK cells (co-transfected with miRNA mimic and PmirGlo Dual Luciferase plasmid) were re-suspended in 150 µL PBS and 10 µL of the suspension was taken to perform luciferase assay using Dual-Glo Luciferase Assay Kit (Promega, E2920) following the manufacturer's protocol. Briefly, the luciferase assay reagent (LAR) was added to the cell suspension. The LAR comprises the lysis solution and the substrate for firefly luciferase protein. After measuring the firefly luciferase activity, a Stop and Glo solution was added which stalled the firefly activity and induced the Renilla luciferase activity. The ratio of firefly/Renilla luciferase activity was calculated and compared between mutated and wild-type (WT) UTR samples for estimating the decline in firefly activity, which reflects the translational repression of the transcripts and thus the miRNA-mediated suppression. Each reaction was set in technical duplicates and at least four biological replicates.

## Generation of transgenic mice

Transgenic mice were generated using non-surgical testicular electroporation as described previously by our laboratory [95]. Briefly, the miR-92a overexpression plasmid DNA which used Rhox5 promoter was prepared in high quantity using GenElute™ HP Plasmid Maxi prep (Sigma Aldrich) and was linearized using StuI restriction enzyme that cuts the plasmid in the backbone. The linearized plasmid was purified by ethanol precipitation and quantified using Nanodrop. The integrity of the linearized DNA was verified by running it on 1% agarose gel. 15 µg of the linearized plasmid DNA at a concentration of 500 ng/µL was injected into each testis of anaesthetized 30 days old FVBJ male mice, followed by electroporation (60 V for 50 ms, 4 forward + 4 reverse pulses) using tweezer electrodes (Electro Square Porator, ECM 830, BTX, USA). The fore-founder animals were housed for 30 days and then mated with age-matched WT females. The pups born (F1 generation) were screened for transgene integration using slot blot analysis (as described below). Several individuals from the F1 generation were transgenic. Infertility was confirmed in F1 generation transgenic males using experiments described below. To continue the transgenic line, WT males and transgenic females from the F1 generation were mated to generate an F2 generation and all experiments were performed on transgenic males from the F2 generation at around 80–90 days of age (Supp. Fig. 2). A control transgenic animal was previously generated by expressing a stem loop-structured shRNA against bacterial LacZ to mimic the pri-microRNA structure, in the same vector backbone. LacZ mice were compared to WT mice to check for any probable effects of transgene overexpression in the animals. As reported previously, no such changes were found between the LacZ control Tg mice and WT mice, and WT was thereafter used as control for all experiments [41].

**Table 2** List of primers used for q-RT-PCR of genes

| Gene | Mouse forward primer | Mouse reverse primer | Rat forward primer | Rat reverse primer |
|---|---|---|---|---|
| 18S | GCAATTATTCCCCATGAACG | GGCCTCACTAAACCATCCAA | -do- | -do- |
| AR | GCCTCCGAAGTGTGGTATCC | GGTACTGTCCAAACGCATGT | CTTATGGGGACATGCGTTTGG | GAGCTCCGTAGTGACAACCA |
| Gja1 | TAAGTGAAAGAGAGGTGCCCAG | CCCAGGAGCAGGATTCTGAAA | GTCTACCCCTCTGGGTGTGA | AGGACCAGTCGAGGATGAT |
| InhbB | CTTCGTCTCTAATGAAGGCAACC | CTCCACCACATTCCACCTGTC | TCCTAGTGCCCTGCTGAGAT | ACCCACAGGGACAACTTCTG |
| Klf4 | CTTGGCCCCGGAAAAGAAC | TTCTCGCCTGTGTGAGTTCG | GTGCCCCGACTAACCGTTG | GTCGTTGAACTCCTCGGTCT |
| Fshr | CCTTGCTCCTGGTCTCCTTG | CTCGGTCACCTTGCTATCTTG | AACGCCATTGAACTGAGGTTTG | GGTTGGAGAACACATCTGCCT |
| Cldn11 | CTCCTTATTCTGCTGGCTCTCT | CATCACAGCACCGATCCAAC | ACGGTTGCGTATGCTTTGA | ACACCCATGAAGCCAAATT |
| KITLG | TCTGCGGGAATCCTGTGACT | CGGCGACATAGTTGAGGGTTAT | GTGGATGACCTCGTGGCATGTA | TCAGATGCCACCATGAAGTCC |
| GDNF | CCGGATCCGAGGTGCC | CCGAGGGAGTGGTCTTCAG | CGCTGACCAGTGACTCCAAT | CGCCGCTTGTTTATCTGGTG |
| ABP | GAACGGGGATTCACTGCTG | GCAGGCACGAGCGGAAA | GACGGACCCTGAGACACATT | AGGGTTTGCTGATTTTGGTG |
| Sox9 | AAGAACGGACAAGCGGAGG | AGATTGCCCAGAGTGCTCG | – | – |
| PTEN | – | – | GCAGAGTTGCACAGTATCC | CCGTCCTTTCCCAGCTTTACA |
| ESR1 | – | – | CGCTCTGCCTTGATCACACA | CGGATGAGCCACCCTGC |
| Sirt1 | – | – | GTTCCAGCCGTCTCTGTGT | GCTGTTGCAAAGGAACCATGA |
| Lats1 | – | – | TGGTGACTCTGGGGATAAAGAA | GGGAGTAACTCTGAATCCGAGAC |
| Tead1 | – | – | GTCCACCAACTCATCACCCG | AACAACCAAACGTGTAGGCAG |
| Rora | – | – | GTGGAGACAAATCGTCAGGAAT | TGGTCCGATCAATCAAACAGTTC |
| miR-92a-OE | TTTTTTTTGAATTCAGACTTCTAGTACTCCTGGATCAAC | TTTTTTTTGTCGACGCTAAAGGATTTTACAATCTTACTATAGCACTG | – | – |
| miR-92a-3p | TCATTCACGGACAACACTTTTT | GCGAGCACAGAATTAATACGAC | TATTGCACTTGTCCCGGCCTG | GCGAGCACAGAATTAATACGAC |

## Genomic DNA isolation and slot blot analysis

Genomic DNA was isolated from 3–4 mm of tail snippets using salt precipitation method [96]. The isolated DNA was quantified using Nanodrop and 1 µg of DNA of each sample was used for slot blot analysis as described previously in our laboratory [95]. Briefly, each genomic DNA sample was denatured at 95 °C for 10 min and immobilized and cross-linked on a positively charged nylon-66 transfer membrane (MDI Membrane Technologies, Ambala Cantt, India, CL-1000 UV crosslinker, UVP). A radioactive DNA probe complementary to the reporter GFP sequence in the plasmid was synthesized by PCR amplifying the GFP coding region. The clean PCR product was denatured and incubated with $\alpha P^{32}$-CTP to produce the radioactive probe. The membrane was hybridized with a $\alpha P^{32}$-CTP radiolabelled probe in a rotating chamber, overnight at 60 °C (Amersham). The membrane was washed gently with low stringency and high stringency 2X SSC (3 M NaCl, 0.3 M sodium citrate, pH 7.0 for 20X SSC) buffer twice for 10 min each and kept in exposure cassettes for 12–24 h, which was then scanned using Phosphorimager Typhoon 9400 (GE Healthcare). Genomic DNA from WT mice was used as negative control and 10 ng of the plasmid (which contained the probe region) was used as a positive control.

**Table 3** List of antibodies used and their dilution

| Antibody | Company | Cat. No | Dilution for IHC |
|---|---|---|---|
| Connexin43 | CST | 3512 | 1:100[a] |
| Claudin11 | Thermo Fisher Scientific | 36–4500 | 1:50[a] |
| PCNA | Thermo Fisher Scientific | MA511358 | 1:100[a] |
| SOX9 | Abcam | ab185230 | 1:100[a] |
| Beta Actin | CST | 4967 | – |
| Anti-mouse alexa 488 | Thermo Fisher Scientific | A11001 | 1:500 |
| Anti-rabbit alexa 488 | Thermo Fisher Scientific | A11008 | 1:500 |

[a]With 1% BSA

## Immunohistochemistry

The freshly collected testes from WT and Tg mice were fixed in 4% paraformaldehyde for 48 h, washed well to remove the fixative and then used for paraffin embedding [97]. 7 µm sections were cut from paraffin embedded blocks and used for immunostaining. The sections were deparaffinized using xylene–alcohol and subjected to antigen unmasking by boiling the sections for 10 min in antigen unmasking solution (Vector Laboratories, H3300) and cooled to room temperature under tap water. The sections were permeabilized by treating them with 0.1% Triton X-100 for 5 min at room temperature, followed by washing with 1X PBS thrice, for 5 min each, and then blocked with 3% BSA solution for 1 h. The sections were then incubated overnight with the primary antibody in 1% BSA at 4 °C in a moist chamber. The primary antibody was removed and sections were washed with 1X PBS to remove any residual antibody and then kept in secondary antibody solution for 3–4 h, washed again and finally stained with 20 µg/mL Hoechst-3342 to stain the nuclei. The sections were mounted on glass slides using prolong gold antifade mounting media (Life Technologies, USA) and viewed under fluorescent microscope (Nikon Eclipse TE2000-E). Primary antibody dilutions are mentioned in Table 3. The fluorescence intensity of the images was quantified using ImageJ. Each tubule was manually outlined using the draw tool and the intensity was measured. This was done for at least four tubules per section (from 20X images) and at least four sections were analysed from three wild-type and three miR-92a-Tg mice.

## Fertility assessment

The fertility assessment was done by measuring parameters such as gonadosomatic index (GSI%), sperm count and litter size in the transgenic and age-matched wild-type mice [41, 98]. The body weight and testis weight for each mice (WT or Tg) were noted and the gonadosomatic index (body weight/testis weight X 100) was calculated. The testis size was also observed for any visible morphological changes. Transgene-positive animals were euthanized at around 80–90 days of age along with their age-matched WT counterparts. The entire intact epididymis was surgically removed and transferred into a 1.5 ml microcentrifuge tube containing 1 ml 1X PBS and ruptured thereafter for sperm count analysis using a haemocytometer. The litter size for each transgene-positive animal was also noted for at least five mating cycles with at least three age-matched females.

## TUNEL assay

Paraffin sections of WT and Tg testis were taken and deparaffinized using xylene and subjected to antigen unmasking using 20 µg/ml proteinase K solution. Apoptosis was detected by performing the TUNEL assay using Promega DeadEnd™ Fluorometric TUNEL System (G3250) as per the manufacturer's protocol [99]. Briefly, the sections were fixed in 4% paraformaldehyde for 20–30 min and then permeabilized using 0.2% Triton X-100 in 1X PBS for 5 min. The sections were then equilibrated and incubated with the enzyme mix containing the fluorophore. The enzyme reaction was stopped using 2X SSC buffer and the sections were stained with 20 µg/mL Hoechst for 5 min, washed and finally preserved using antifade (Prolong Gold antifade, Invitrogen). Slides were viewed under fluorescent microscope (Nikon Eclipse TE2000-E) to detect fluorescent TUNEL-positive cells.

## Transmission electron microscopy

Whole testis from WT and transgene-positive animals were fixed in 2% paraformaldehyde + 2.5% glutaraldehyde in 0.1 m phosphate buffer solution, for 6–8 h and cut into small pieces of approximately 2 X 2 mm dimension. These pieces were washed once with 1X PBS and incubated for 1 h in osmium tetroxide for secondary fixation. The tissue was dehydrated using ethanol and infiltrated using epoxy resin, which was allowed to settle and polymerize at 60 °C overnight. Ultrathin sections of approximately 70 nm were cut at Sophisticated Analytical Instrumentation Facility, All India Institute of Medical Science, New Delhi. TEM imaging was

done (Tecnai G2 20 Twin) at the National Institute of Immunology, New Delhi.

### Protein extraction and immunoblot analysis

Protein was extracted from the tissue by homogenizing it in RIPA lysis buffer (with 1X Protease and phosphatase inhibitor cocktail). Protein was quantified using Bradford solution [100] and 20–30 µg total protein was run on 12% resolving SDS PAGE gel at 100 mV. The protein was transferred onto PVDF membranes and incubated with blocking solution (5% skimmed non-fat milk in 1X TBST) for 1 h at room temperature. The membrane was briefly washed with 1 X TBST and incubated overnight with the primary CX43 antibody (CST-3512, at 1:1000) dissolved in 1X TBST. The next day, the membrane was washed thrice with 1X TBST (5 min each at RT under rapid shaking condition) and incubated for an hour with the HRP-labelled secondary antibody (1:5000) in 1X TBST. The membrane was then developed using BioRad Clarity Western ECL substrate and imaged in a chemi-doc (ImageQuant Las 500, GE Healthcare). The protein bands obtained were quantified using ImageJ. β-actin was used as loading control (CST-4967, 1:1000).

### Statistical analysis

Statistical analysis was performed using GraphPad Prism 8.2 software. Data (mean ± SEM) from at least three independent experiments was used for calculating statistical significance. Details of the statistical tests are provided in the figure legends. $p$ value < 0.05 was considered to be statistically significant, where * = $p < 0.05$, ** = $p < 0.01$, *** = $p < 0.001$, **** = $p < 0.0001$.

**Supplementary Information** The online version contains supplementary material available at https://doi.org/10.1007/s00018-022-04174-9.

**Acknowledgements** We are grateful to the Director of National Institute of Immunology, for the valuable support. We thank Prof. Miles F. Wilkinson, University of California, San Diego, USA, for providing proximal Rhox 5 promoter. We greatly acknowledge the technical support from Dr. Parminder Singh (NII, New Delhi) and Mr. Birendra N. Roy (NII, New Delhi). We acknowledge the help of Dr. Souvik Sen Sharma (NIAB, Hyderabad) for editing the manuscript. We acknowledge the help from the staff of Small Animal Facility of National Institute of Immunology.

**Author contributions** AG, KM and SSM conceptualized the study. AG, KM and SSM designed the experiments. AG performed most experiments with help from AV, AGH and RS. AG, KM, IB and SSM analysed the experimental data. AG, IB and SSM wrote the manuscript. All authors contributed to the article and approved the submitted version.

**Funding** We acknowledge the financial support provided by the Department of Biotechnology, Government of India, under a core fund through the National Institute of Immunology. We also acknowledge financial support from JC Bose fellowship of SSM (SERB-JCB/2017/000027) for this work.

**Data availability** Not applicable.

**Code availability** Not applicable.

## Declarations

**Conflict of interest** The authors declare no competing interest.

**Ethical approval** Included in "Materials and methods".

**Consent to participate** Not applicable.

## References

1. Irvine DS (1998) Epidemiology and aetiology of male infertility. Human Reprod (Oxford, England) 13(Suppl 1):33–44
2. Sharpe RM (2012) Sperm counts and fertility in men: a rocky road ahead. Science & society series on sex and science. EMBO Rep 13:398–403. https://doi.org/10.1038/embor.2012.50
3. Agarwal A, Baskaran S, Parekh N et al (2021) Male infertility. Lancet 397:319–333. https://doi.org/10.1016/S0140-6736(20)32667-2
4. Ravitsky V, Kimmins S (2019) The forgotten men: rising rates of male infertility urgently require new approaches for its prevention, diagnosis and treatment. Biol Reprod 101:872–874. https://doi.org/10.1093/BIOLRE/IOZ161
5. Thirumavalavan N, Gabrielsen JS, Lamb DJ (2019) Where are we going with gene screening for male infertility? Fertil Steril 111:842–850
6. Alves MBR, Celeghini ECC, Belleannée C (2020) From sperm motility to sperm-borne microRNA signatures: new approaches to predict male fertility potential. Front Cell Develop Biol 8:791
7. Jung JH, Seo JT (2014) Empirical medical therapy in idiopathic male infertility: promise or panacea? Clin Exp Reprod Med 41:108–114. https://doi.org/10.5653/cerm.2014.41.3.108
8. Matzuk MM, Lamb DJ (2008) The biology of infertility: research advances and clinical challenges. Nat Med 14:1197–1213
9. Majumdar SS, Winters SJ, Plant TM (1997) A study of the relative roles of follicle-stimulating hormone and luteinizing hormone in the regulation of testicular inhibin secretion in the Rhesus monkey (*Macaca mulatta*). Endocrinology 138:1363–1373. https://doi.org/10.1210/endo.138.4.5058
10. Bhattacharya I, Sen Sharma S, Majumdar SS (2019) Pubertal orchestration of hormones and testis in primates. Mol Reprod Dev 86:1505–1530
11. Smith LB, Walker WH (2014) The regulation of spermatogenesis by androgens. Semin Cell Dev Biol 30:2–13
12. Walker WH, Cheng J (2005) FSH and testosterone signaling in Sertoli cells. Reproduction 130:15–28. https://doi.org/10.1530/rep.1.00358
13. Griswold MD (2018) 50 years of spermatogenesis: Sertoli cells and their interactions with germ cells. Biol Reprod 99:87–100
14. França LR, Hess RA, Dufour JM et al (2016) The Sertoli cell: one hundred fifty years of beauty and plasticity. Andrology 4:189–212. https://doi.org/10.1111/andr.12165
15. Cheng CY, Wong EWP, Lie PPY et al (2011) Regulation of blood-testis barrier dynamics by desmosome, gap junction, hemidesmosome and polarity proteins. Spermatogenesis 1:105–115. https://doi.org/10.4161/spmg.1.2.15745

16. Orth JM, Gunsalus GL, Lamperti AA (1988) Evidence from Sertoli cell-depleted rats indicates that spermatid number in adults depends on numbers of Sertoli cells produced during perinatal development. Endocrinology 122:787–794. https://doi.org/10.1210/endo-122-3-787
17. Bhattacharya I, Basu S, Sarda K et al (2015) Low levels of gαs and Ric8b in testicular Sertoli cells may underlie restricted FSH action during infancy in primates. Endocrinology 156:1143–1155. https://doi.org/10.1210/en.2014-1746
18. Bhattacharya I, Pradhan BS, Sarda K et al (2012) A switch in Sertoli cell responsiveness to FSH may be responsible for robust onset of germ cell differentiation during prepubartal testicular maturation in rats. Am J Physiol-Endocrinol Metab 303:E886–E898. https://doi.org/10.1152/ajpendo.00293.2012
19. Bhattacharya I, Basu S, Pradhan BS et al (2019) Testosterone augments FSH signaling by upregulating the expression and activity of FSH-receptor in pubertal primate Sertoli cells. Mol Cell Endocrinol 482:70–80. https://doi.org/10.1016/j.mce.2018.12.012
20. Chalmel F, Rolland AD (2015) Linking transcriptomics and proteomics in spermatogenesis. Reproduction 150:R149–R157
21. Zimmermann C, Stévant I, Borel C et al (2015) Research resource: the dynamic transcriptional profile of Sertoli cells during the progression of spermatogenesis. Mol Endocrinol 29:597–612. https://doi.org/10.1210/me.2014-1356
22. Gautam M, Bhattacharya I, Rai U, Majumdar SS (2018) Hormone induced differential transcriptome analysis of Sertoli cells during postnatal maturation of rat testes. PLoS ONE 13:e0191201. https://doi.org/10.1371/journal.pone.0191201
23. Soffientini U, Rebourcet D, Abel MH et al (2017) Identification of Sertoli cell-specific transcripts in the mouse testis and the role of FSH and androgen in the control of Sertoli cell activity. BMC Genom. https://doi.org/10.1186/s12864-017-4357-3
24. Mandal K, Bader SL, Kumar P et al (2017) An integrated transcriptomics-guided genome-wide promoter analysis and next-generation proteomics approach to mine factor(s) regulating cellular differentiation. DNA Res 24:dsw057. https://doi.org/10.1093/dnares/dsw057
25. Majumdar SS, Bhattacharya I (2013) Genomic and post-genomic leads toward regulation of spermatogenesis. Prog Biophys Mol Biol 113:409–422. https://doi.org/10.1016/j.pbiomolbio.2013.01.002
26. Tilbrook AJ, Clarke IJ (2001) Negative feedback regulation of the secretion and actions of gonadotropin-releasing hormone in males. Biol Reprod 64:735–742. https://doi.org/10.1095/biolreprod64.3.735
27. Carthew RW, Sontheimer EJ (2009) Origins and mechanisms of miRNAs and siRNAs. Cell 136:642–655. https://doi.org/10.1016/J.CELL.2009.01.035
28 Wahid F, Shehzad A, Khan T, Kim YY (2010) MicroRNAs: synthesis, mechanism, function, and recent clinical trials. Biochimica et Biophysica Acta Mol Cell Res 1803:1231–1243. https://doi.org/10.1016/J.BBAMCR.2010.06.013
29. Nakanishi K (2016) Anatomy of RISC: how do small RNAs and chaperones activate Argonaute proteins? Wiley Interdiscip Rev RNA 7:637–660. https://doi.org/10.1002/wrna.1356
30. Kim G-J, Georg I, Scherthan H et al (2010) Dicer is required for Sertoli cell function and survival. Int J Dev Biol 54:867–875. https://doi.org/10.1387/ijdb.092874gk
31. Papaioannou MD, Pitetti J-L, Ro S et al (2009) Sertoli cell Dicer is essential for spermatogenesis in mice. Dev Biol 326:250–259. https://doi.org/10.1016/j.ydbio.2008.11.011
32. Papaioannou MD, Lagarrigue M, Vejnar CE et al (2011) Loss of Dicer in Sertoli cells has a major impact on the testicular proteome of mice. Mol Cell Proteom 10:M900587–M901200. https://doi.org/10.1074/mcp.M900587-MCP200
33. Wu Q, Song R, Ortogero N et al (2012) The RNase III enzyme DROSHA is essential for microRNA production and spermatogenesis. J Biol Chem 287:25173–25190. https://doi.org/10.1074/jbc.M112.362053
34. Wu J, Bao J, Kim M et al (2014) Two miRNA clusters, miR-34b/c and miR-449, are essential for normal brain development, motile ciliogenesis, and spermatogenesis. Proc Natl Acad Sci USA. https://doi.org/10.1073/pnas.1407777111
35. Gao H, Wen H, Cao C et al (2019) Overexpression of MicroRNA-10a in germ cells causes male infertility by targeting Rad51 in mouse and human. Front Physiol 10:765. https://doi.org/10.3389/fphys.2019.00765
36. Lian J, Tian H, Liu L et al (2010) Downregulation of microRNA-383 is associated with male infertility and promotes testicular embryonal carcinoma cell proliferation by targeting IRF1. Cell Death Dis 1:94. https://doi.org/10.1038/cddis.2010.70
37. Cheng YS, Chung CL, Chen CF, Lin YM (2017) Differential expression of microRNAs and their messengerRNA targets in men with normal spermatogenesis versus Sertoli cell-only syndrome. Urol Sci 28:42–49. https://doi.org/10.1016/J.UROLS.2016.03.002
38. Luo L, Ye L, Liu G et al (2010) Microarray-based approach identifies differentially expressed MicroRNAs in porcine sexually immature and mature testes. PLoS ONE 5:e11744. https://doi.org/10.1371/journal.pone.0011744
39. Yan N, Lu Y, Sun H et al (2009) Microarray profiling of microRNAs expressed in testis tissues of developing primates. J Assist Reprod Genet 26:179–186. https://doi.org/10.1007/s10815-009-9305-y
40. Aliberti P, Sethi R, Belgorosky A et al (2019) Gonadotrophin-mediated miRNA expression in testis at onset of puberty in rhesus monkey: predictions on regulation of thyroid hormone activity and DLK1-DIO3 locus. Mol Hum Reprod 25:124–136. https://doi.org/10.1093/molehr/gay054
41. Gupta A, Mandal K, Singh P et al (2021) Declining levels of miR-382-3p at puberty triggers the onset of spermatogenesis. Mol Ther Nucleic Acids. https://doi.org/10.1016/J.OMTN.2021.07.001
42. Jiang M, Li X, Quan X et al (2019) MiR-92a family: a novel diagnostic biomarker and potential therapeutic target in human cancers. Front Mol Biosci 6:98. https://doi.org/10.3389/fmolb.2019.00098
43. Mogilyansky E, Rigoutsos I (2013) The miR-17/92 cluster: a comprehensive update on its genomics, genetics, functions and increasingly important and numerous roles in health and disease. Cell Death Differ 20:1603–1614
44 Huhtaniemi I (2015) A short evolutionary history of FSH-stimulated spermatogenesis. Hormones 14:468–478. https://doi.org/10.14310/horm.2002.1632
45. Crépieux P, Marion S, Martinat N et al (2001) The ERK-dependent signalling is stage-specifically modulated by FSH, during primary Sertoli cell maturation. Oncogene 20:4696–4709. https://doi.org/10.1038/sj.onc.1204632
46. Meachem SJ, Ruwanpura SM, Ziolkowski J et al (2005) Developmentally distinct in vivo effects of FSH on proliferation and apoptosis during testis maturation. J Endocrinol 186:429–446. https://doi.org/10.1677/joe.1.06121
47. Orth JM (1984) The role of follicle-stimulating hormone in controlling sertoli cell proliferation in testes of fetal rats. Endocrinology 115:1248–1255. https://doi.org/10.1210/endo-115-4-1248
48. Rebourcet D, Darbey A, Monteiro A et al (2017) Sertoli cell number defines and predicts germ and leydig cell population sizes in the adult mouse testis. Endocrinology 158:2955–2969. https://doi.org/10.1210/EN.2017-00196
49. Xiong C (2014) Identification of microRNAs predominately derived from testis and epididymis in human seminal plasma.

Clin Biochem 47:967–972. https://doi.org/10.1016/j.clinbiochem.2013.11.009
50. Yan N, Lu Y, Sun H et al (2007) A microarray for microRNA profiling in mouse testis tissues. Reproduction 134:73–79. https://doi.org/10.1530/REP-07-0056
51. Buchold GM, Coarfa C, Kim J et al (2010) Analysis of MicroRNA expression in the prepubertal testis. PLoS ONE 5:e15317. https://doi.org/10.1371/journal.pone.0015317
52. Panneerdoss S, Chang Y-F, Buddavarapu KC et al (2012) Androgen-responsive MicroRNAs in mouse Sertoli cells. PLoS ONE 7:e41146. https://doi.org/10.1371/journal.pone.0041146
53 León K, Gallay N, Poupon A et al (2013) Integrating microRNAs into the complexity of gonadotropin signaling networks. Front Cell Develop Biol 1:3. https://doi.org/10.3389/fcell.2013.00003
54. Yao N, Yang BQ, Liu Y et al (2010) Follicle-stimulating hormone regulation of microRNA expression on progesterone production in cultured rat granulosa cells. Endocrine 38:158–166. https://doi.org/10.1007/s12020-010-9345-1
55. Lu C, Shan Z, Hong J, Yang L (2017) MicroRNA-92a promotes epithelial-mesenchymal transition through activation of PTEN/PI3K/AKT signaling pathway in non-small cell lung cancer metastasis. Int J Oncol 51:235–244. https://doi.org/10.3892/ijo.2017.3999
56. Zhang G, Zhou H, Xiao H et al (2014) MicroRNA-92a functions as an oncogene in colorectal cancer by targeting PTEN. Dig Dis Sci. https://doi.org/10.1007/s10620-013-2858-8
57. Li X, Guo S, Min L et al (2019) MiR-92a-3p promotes the proliferation, migration and invasion of esophageal squamous cell cancer by regulating PTEN. Int J Mol Med 44:973–981. https://doi.org/10.3892/ijmm.2019.4258
58. Liu Y, Hu Q, Ao J et al (2020) Role of miR-92a-3p/PTEN axis in regulation of pancreatic cancer cell proliferation and metastasis. J Cent South Univ (Med Sci) 45:280–289. https://doi.org/10.11817/j.issn.1672-7347.2020.180459
59. Liu P, Su J, Song X, Wang S (2018) MiR-92a regulates the expression levels of matrix metalloproteinase 9 and tissue inhibitor of metalloproteinase 3 via sirtuin 1 signaling in hydrogen peroxide-induced vascular smooth muscle cells. Mol Med Rep 17:1041–1048. https://doi.org/10.3892/mmr.2017.7937
60. Chen Z, Shentu TP, Wen L et al (2013) Regulation of SIRT1 by oxidative stress-responsive miRNAs and a systematic approach to identify its role in the endothelium. Antioxid Redox Signal 19:1522–1538
61. Howard EW, Yang X (2018) MicroRNA regulation in estrogen receptor-positive breast cancer and endocrine therapy. Biol Proced Online 20:17
62. Wu S, Yan M, Ge R, Cheng CY (2020) Crosstalk between Sertoli and germ cells in male fertility. Trends Mol Med 26:215–231
63. Morrow CMK, Mruk D, Cheng CY, Hess RA (2010) Claudin and occludin expression and function in the seminiferous epithelium. Philos Transact R Soc B 365:1679–1696
64. Hakovirta H, Yan W, Kaleva M et al (1999) Function of stem cell factor as a survival factor of spermatogonia and localization of messenger ribonucleic acid in the rat seminiferous epithelium. Endocrinology 140:1492–1498. https://doi.org/10.1210/endo.140.3.6589
65. Parekh PA, Garcia TX, Hofmann MC (2019) Regulation of GDNF expression in Sertoli cells. Reproduction 157:R95–R107
66. Rao MK, Wayne CM, Meistrich ML, Wilkinson MF (2003) Pem homeobox gene promoter sequences that direct transcription in a Sertoli cell-specific, stage-specific, and androgen-dependent manner in the testis in vivo. Mol Endocrinol 17:223–233. https://doi.org/10.1210/me.2002-0232
67. Pradhan BS, Bhattacharya I, Sarkar R, Majumdar SS (2020) Pubertal down-regulation of Tetraspanin 8 in testicular Sertoli cells is crucial for male fertility. Mol Hum Reprod 26:760–772. https://doi.org/10.1093/molehr/gaaa055
68. Pradhan BS, Bhattacharya I, Sarkar R, Majumdar SS (2019) Downregulation of Sostdc1 in testicular Sertoli cells is prerequisite for onset of robust spermatogenesis at puberty. Sci Rep 9:1–11. https://doi.org/10.1038/s41598-019-47930-x
69. Bhardwaj A, Song HW, Beildeck M et al (2012) DNA demethylation-dependent AR recruitment and GATA factors drive Rhox5 homeobox gene transcription in the epididymis. Mol Endocrinol 26:538–549. https://doi.org/10.1210/ME.2011-1059
70. Sharpe RM, McKinnell C, Kivlin C, Fisher JS (2003) Proliferation and functional maturation of Sertoli cells, and their relevance to disorders of testis function in adulthood. Reproduction (Cambridge, England) 125:769–784
71. Walker WH (2003) Molecular mechanisms controlling Sertoli cell proliferation and differentiation. Endocrinology 144:3719–3721. https://doi.org/10.1210/en.2003-0765
72. Hai Y, Hou J, Liu Y et al (2014) The roles and regulation of Sertoli cells in fate determinations of spermatogonial stem cells and spermatogenesis. Semin Cell Dev Biol 29:66–75. https://doi.org/10.1016/j.semcdb.2014.04.007
73. Ma M, Yang S, Zhang Z et al (2013) Sertoli cells from non-obstructive azoospermia and obstructive azoospermia patients show distinct morphology, Raman spectrum and biochemical phenotype. Hum Reprod 28:1863–1873. https://doi.org/10.1093/HUMREP/DET068
74. Plotton I, Sanchez P, Durand P, Lejeune H (2006) Decrease of both stem cell factor and clusterin mRNA levels in testicular biopsies of azoospermic patients with constitutive or idiopathic but not acquired spermatogenic failure. Hum Reprod 21:2340–2345. https://doi.org/10.1093/HUMREP/DEL158
75. Tesarik J, Bahceci M, Özcan C et al (1999) Restoration of fertility by in-vitro spermatogenesis. Lancet 353:555–556. https://doi.org/10.1016/S0140-6736(98)04784-9
76. Schaison G, Young J, Pholsena M et al (1993) Failure of combined follicle-stimulating hormone-testosterone administration to initiate and/or maintain spermatogenesis in men with hypogonadotropic hypogonadism. J Clin Endocrinol Metab 77:1545–1549. https://doi.org/10.1210/JCEM.77.6.8263139
77. Oduwole OO, Peltoketo H, Huhtaniemi IT (2018) Role of follicle-stimulating hormone in spermatogenesis. Front Endocrinol 9:763
78 Kaitu'u-Lino TJ, Sluka P, Foo CFH, Stanton PG (2007) Claudin-11 expression and localisation is regulated by androgens in rat Sertoli cells in vitro. Reproduction 133:1169–1179. https://doi.org/10.1530/REP-06-0385
79. Verhoeven G, Cailleau J (1988) Follicle-stimulating hormone and androgens increase the concentration of the androgen receptor in sertoli cells. Endocrinology 122:1541–1550. https://doi.org/10.1210/endo-122-4-1541
80. Block LJ, Mackenbach P, Trapman J et al (1989) Follicle-stimulating hormone regulates androgen receptor mRNA in Sertoli cells. Mol Cell Endocrinol 63:267–271. https://doi.org/10.1016/0303-7207(89)90104-4
81. Sanborn BM, Caston LA, Chang C et al (1991) Regulation of androgen receptor mRNA in rat Sertoli and peritubular cells. Biol Reprod 45:634–641. https://doi.org/10.1095/BIOLREPROD45.4.634
82. Mazaud-Guittot S, Meugnier E, Pesenti S et al (2010) Claudin 11 deficiency in mice results in loss of the Sertoli cell epithelial phenotype in the testis. Biol Reprod 82:202–213. https://doi.org/10.1095/biolreprod.109.078907
83. Brehm R, Zeiler M, Rüttinger C et al (2007) A sertoli cell-specific knockout of connexin43 prevents initiation of spermatogenesis. Am J Pathol 171:19–31. https://doi.org/10.2353/ajpath.2007.061171

84. Behr R, Kaestner KH (2002) Developmental and cell type-specific expression of the zinc finger transcription factor Krüppel-like factor 4 (Klf4) in postnatal mouse testis. Mech Dev 115:167–169. https://doi.org/10.1016/S0925-4773(02)00127-2
85. Godmann M, Kosan C, Behr R (2010) Krüppel-like factor 4 is widely expressed in the mouse male and female reproductive tract and responds as an immediate early gene to activation of the protein kinase a in TM4 Sertoli cells. Reproduction 139:771–782. https://doi.org/10.1530/REP-09-0531
86. Godmann M, Gashaw I, Katz JP et al (2009) Krüppel-like factor 4, a "pluripotency transcription factor" highly expressed in male postmeiotic germ cells, is dispensable for spermatogenesis in the mouse. Mech Dev 126:650–664. https://doi.org/10.1016/j.mod.2009.06.1081
87. Godmann M, Katz JP, Guillou F et al (2008) Krüppel-like factor 4 is involved in functional differentiation of testicular Sertoli cells. Dev Biol 315:552–566. https://doi.org/10.1016/j.ydbio.2007.12.018
88. Lv H, Zhang Z, Wang Y et al (2016) MicroRNA-92a promotes colorectal cancer cell growth and migration by inhibiting KLF4. Oncol Res 23:283–290. https://doi.org/10.3727/096504016X14562725373833
89. Behr R, Deller C, Godmann M et al (2007) Krüppel-like factor 4 expression in normal and pathological human testes. Mol Hum Reprod 13:815–820. https://doi.org/10.1093/molehr/gam064
90. Welsh MJ, Wiebe JP (1975) Rat Sertoli cells: a rapid method for obtaining viable cells. Endocrinology 96:618–624. https://doi.org/10.1210/endo-96-3-618
91. Bhattacharya I, Gautam M, Sarkar H et al (2017) Advantages of pulsatile hormone treatment for assessing hormone-induced gene expression by cultured rat Sertoli cells. Cell Tissue Res 368:389–396. https://doi.org/10.1007/s00441-016-2410-1
92. Chomczynski P, Sacchi N (1987) Single-step method of RNA isolation by acid guanidinium thiocyanate-phenol-chloroform extraction. Anal Biochem 162:156–159. https://doi.org/10.1016/0003-2697(87)90021-2
93. Schmittgen TD, Livak KJ (2008) Analyzing real-time PCR data by the comparative CT method. Nat Protoc 3:1101–1108. https://doi.org/10.1038/nprot.2008.73
94. Kuchipudi SV, Tellabati M, Nelli RK et al (2012) 18S rRNA is a reliable normalisation gene for real time PCR based on influenza virus infected cells. Virol J 9:230. https://doi.org/10.1186/1743-422X-9-230
95. Usmani A, Ganguli N, Sarkar H et al (2013) A non-surgical approach for male germ cell mediated gene transmission through transgenesis. Sci Rep 3:1–8. https://doi.org/10.1038/srep03430
96. El-Ashram S, Al Nasr I, Suo X (2016) Nucleic acid protocols: extraction and optimization. Biotechnol Rep 12:33–39. https://doi.org/10.1016/j.btre.2016.10.001
97. Crosby K, Simendinger J, Grange C, et al (2014) Immunohistochemistry protocol for paraffin-embedded tissue sections—protocol. https://www.jove.com/t/5064/immunohistochemistry-protocol-for-paraffin-embedded-tissue-sections. Accessed 14 Apr 2021
98. Sarkar RK, Sen Sharma S, Mandal K et al (2021) Homeobox transcription factor Meis1 is crucial to Sertoli cell mediated regulation of male fertility. Andrology 9:689–699. https://doi.org/10.1111/andr.12941
99. Kyrylkova K, Kyryachenko S, Leid M, Kioussi C (2012) Detection of apoptosis by TUNEL assay. Methods Mol Biol 887:41–47. https://doi.org/10.1007/978-1-61779-860-3_5
100 Kruger NJ (2002) The Bradford method for protein quantitation. In: Walker JM (ed) The protein protocols handbook. Humana Press, New Jersey, pp 15–21